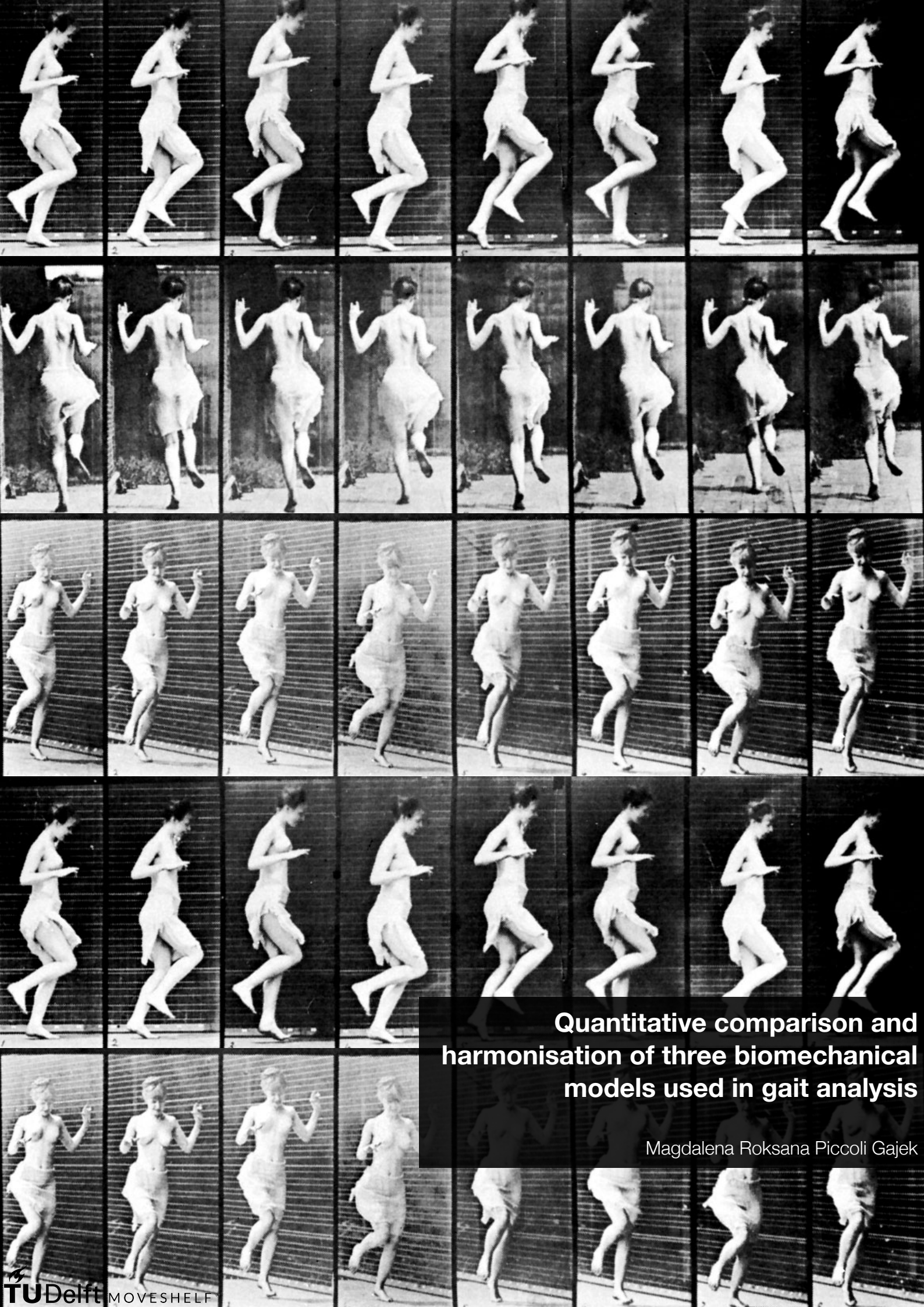

Quantitative comparison and harmonisation of three biomechanical models used in gait analysis

Magdalena Roksana Piccoli Gajek

TU Delft MOVESHELF

Quantitative comparison and harmonisation of three biomechanical models used in gait analysis

Master Thesis in Biomedical Engineering
BM51032

by

Magdalena Roksana Piccoli Gajek
4938275

Department of Biomechanical Engineering
Faculty of Mechanical, Maritime and Material Engineering
Delft University of Technology
BioMechaMotion Lab
In collaboration with Moveshelf Labs B.V.

MOVESHELF®

To be defended on January 15th, 2021

Thesis Committee: Prof. dr. ir. Jaap Harlaar
Dr. ir. Ignazio Aleo
Prof. dr. DirkJan Veeger
Dr. Manon Kok

Contents

Abstract

INTRODUCTION: Clinical gait analysis is used to assess patients' impairments, improve treatment decision-making and monitor patients' progress. Motion capture of markers placed on the skin is the gold standard technique for gait analysis. Markers referenced to the underlying bones are used to define a biomechanical model, i.e. an anatomical frame for each body segment. Several biomechanical models have been proposed, and none can be considered as ground truth. The outcomes from different biomechanical models provide non comparable data, this hampers data sharing and impedes the full potential of clinical interpretation and treatment recommendation.

OBJECTIVES: This study explores the differences in biomechanical models' definitions used for gait analysis and evaluates four harmonisation techniques with the aim to improve kinematic data comparability.

METHODS: Nine healthy participants performed a walking task. A merged markerset was developed by including three widely adopted biomechanical models: CGM, CAST and LAMB. The harmonisation processes involved three coordinate transformations between anatomical frames based on the calibration trial, the mean of the task trial and the frame-by-frame of the task trial. The fourth harmonisation consisted in inverse kinematics fitting based on the same underlying model (OpenSim). Differences before and after each harmonisation approach were analysed by considering joint kinematics.

RESULTS: The differences between the native biomechanical models' definitions reach 23.2° of rotation and 41mm of translation. A systematic difference between models was found, which was higher than between subjects, and varied across the gait cycle with a nonlinear pattern. All harmonisation processes improved kinematic data comparability. No statistically significant difference between the curves was found when results were harmonised with frame-by-frame coordinate transformation. Harmonisation based on inverse kinematics provides comparable results, with the exception of ankle parameters on sagittal plane.

DISCUSSION: The nonlinear and gait cycle-dependent systematic difference between biomechanical models is suggested to be due to the soft tissue artefact. As soft tissue artefact varies across the gait cycle and between subjects, it is reasonable that a frame-by-frame harmonisation provides more comparable results, as the dynamic transformation takes into account the nonlinear soft tissue behavior. However, it remains specific for gait.

CONCLUSION: This study provides promising methodologies for kinematic data harmonisation and allows to easily switch between biomechanical models without gaining consensus on which biomechanical model should be mostly used. However, further investigation of soft tissue artefact effects on biomechanical models' definitions and consequent joint kinematics is still required to approximate the ground truth.

List of abbreviations

AF	Anatomical Frame
AIM	Automatic Identification of Markers
AJC	Ankle Joint Center
AL	Anatomical Landmark (marker)
CAST	Calibrated Anatomical System Technique
CGM	Conventional Gait Model
CS	Coordinate System
CT	Coordinate Transformation
DK	Direct Kinematics
DoF	Degree of Freedom
GF	Global Frame
HBM	Human Body Model
HJC	Hip Joint Center
IC	Initial Contact
IK	Inverse Kinematics
KJC	Knee Joint Center
LAMB	Laboratorio di Analisi del Movimento del Bambino
MCID	Minimal Clinically Important Difference
PiG	Plug-in-Gait
QTM	Qualisys Track Manager
RMSE	Root Mean Square Error
ROM	Range of Motion
SD	Standard Deviation
SPE	Statistical Parametric Mapping
STA	Soft Tissue Artefact
TF	Technical Frame
TM	Technical Marker

List of Figures

List of Tables

1 Introduction

1.1 Background

Motion analysis represents a technique to collect quantitative information about the mechanics of the musculoskeletal system while performing a physical activity. Quantitative data is used in medicine, sport, entertainment and security. In particular, in a clinical context, motion data is used to improve clinical decision-making and to monitor patients progress [1]. Gait analysis consists in human walking assessment, typically, by comparison between normal and abnormal walking patterns and to assess changes over time [2].

Marker-based motion capture is the non-invasive gold standard technique for gait analysis. It consists of 3D reconstruction of reflective markers position, placed on the surface of the human body, through stereophotogrammetric cameras [2, 3, 4, 5]. There are two approaches to calculate joint kinematics from marker trajectory data: direct and inverse kinematics.

Direct Kinematics

In the direct kinematics (DK) approach (Figure 1), markers are used to define a *biomechanical model* to calculate outcome measures, such as joints angles kinematics [6, 7].

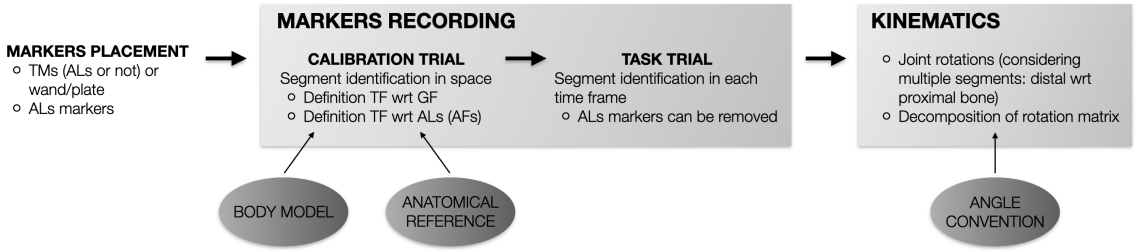

Figure 1: DK workflow.

A biomechanical model consists of coordinate systems (CS) definitions for each body segment – anatomical frames (AFs), joint centers estimations, and the relationships between adjacent AFs to compute joint angles. To define a CS at least three markers are needed [8]. AFs are based on anatomical landmark markers (ALs) – markers placed on bony prominences usually identified by manual palpation. ALs require accurate and repeatable markers placement. AFs approximate anatomical planes, which allow to correlate the movement according to anatomical definitions, thus, easier clinical interpretation [2, 3]. However, as some ALs are not easily seen by the cameras, can fall during walking or are positioned on a highly wobbling soft tissue (i.e. soft tissue artefact – STA – movement between the marker mounted on the subject skin and the underlying bone [9, 10]), technical markers (TMs) are used to provide markers redundancy [3, 8]. TMs define technical frames (TFs) and allow to remove problematic ALs after the calibration trial, thanks to the procedure called *anatomical landmark calibration* [11]. In particular, during the task trials, ALs can be reconstructed in the TFs, based on the assumption that the AL position does

not shift with respect to the TF [8]. Therefore, TMs are recorded during the task trial and ALs position is reconstructed in each frame, based on the anatomical calibration performed during the calibration trial [11, 12]. For details see Appendix A.

Among the existing biomechanical models, *Conventional Gait Model* (CGM) [13, 14] is the oldest and most commonly used, especially because it uses minimised markerset and it is included in the commercially available software Vicon Nexus, as Plug-in-Gait model (PiG – Vicon Motion Systems, Oxford, UK). *Calibrated Anatomical System Technique* (CAST) [8, 11, 15] has been proposed to standardise gait analysis marker-based technique and it is considered more as a set of requirements for proper model construction. CAST is highly based on TMs and anatomical calibration. This model is implemented in the open source BodyMech software (Dep. of Rehabilitation Medicine, VUmc, Amsterdam, The Netherlands). *Laboratorio di Analisi del Movimento del Bambino* (LAMB) [16] is a more recently developed model with the focus on skin markers only. The aim of this model is to assure patients collaboration and to improve inter-operators variability.

Inverse Kinematics

The second approach (Figure 2) to calculate the outcome measures consists in inverse kinematics (IK), also known as global optimisation or kinematic fitting [2]. The human body is modelled with rigid segments linked by joints. First, the model's segment dimensions are adjusted to the specific subject, based on the static trial. Then, the optimal position of the model is calculated by applying joint angles to fit best the task trial measured marker data by minimising a cost function [17, 18]. The advantages of this method are: it can describe any biomechanical model and anatomy, offers more flexibility in markers placement and minimises STA [2, 9, 17, 19, 20]. Moreover, it allows for subject-specific musculoskeletal analysis and simulation, which may help to identify causes of dysfunction, and treatment planning. Therefore, it may improve clinical decision-making and patients' outcomes [18, 21]. IK is incorporated in the open source musculoskeletal modelling software OpenSim [18, 22], and Human Body Model (HBM) [23], implemented in GOAT (Motekforce Link B.V., Amsterdam, The Netherlands). Several OpenSim IK models exist, but according to *Roelker et al.* [24], Gait2392 [25], with 3-1-1 DoFs on the hip, knee and ankle respectively, is accurate enough to assess healthy subjects walking.

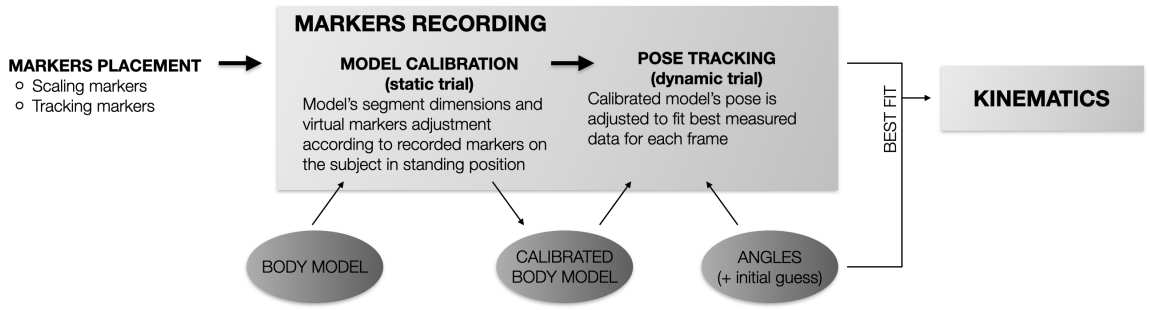

Figure 2: IK workflow.

1.2 Problem Definition

Although all the biomechanical models share the same main purpose – provide accurate and repeatable gait measurements – they all differ in definitions and joint centers estimations. Consequently, their outcome measures are difficult to compare, especially knee and ankle joint angles on frontal and transverse planes, as shown extensively by the literature [26, 27, 28, 29, 30]. This hampers data sharing due to the reduced repeatability and comparability [3, 26], which is already highly affected by the following factors: instrumental error [4]; subject-, task- and marker position-dependent STA [9, 10, 31]; inter- and intra- subjects intrinsic variability and inter- and intra- operators inconsistencies in marker placement [32]. As a detrimental consequence, these different variability sources interfere with clinical interpretation and treatment recommendation [27, 32]. Moreover, clinical laboratories avoid using different models due to these comparability issues, which further hinders innovation and development in gait analysis.

Commercially available biomechanical models or their custom modifications are frequently used [26]. Intra-model repeatability is high, while inter-models variability is reported to be higher than inter-operators [27]. When considering gait analysis outcomes from different laboratories, the outcomes are usually analysed with respect to inter- and intra- trials and operators variabilities [12, 26]. Different markersets and biomechanical models are not always adequately reported in comparison studies and the role of different biomechanical models' definitions in the outcome calculations is insufficiently considered.

The outcome repeatability between different biomechanical models has been assessed by a limited number of studies: *Ferrari et al.* [27] and *Flux et al.* [30], on healthy and cerebral palsy participants, respectively. The uniqueness of both of these studies consists in the use of a merged markerset, accounting for different models included in the analysis. The merged markerset allows to exclude inter-trials variability and minimize inter- and intra- operators variability. Thus, outcomes from different biomechanical models are obtained for the exact same gait cycle and the variability is associated only with the biomechanical models. *Flux et al.* [30] concluded that there are significant inconsistencies when different models are implemented, with the difference being up to 25° on out-of-sagittal planes. In particular, *Ferrari et al.* [27] reported opposite patterns in out-of-sagittal planes kinematics and a knee abduction up to 30°, calculated with CGM, for a patient with a knee prosthesis restraining this rotation (i.e. it should be 0°). The opposite waveform pattern is also observed in inter-laboratory comparison study of *Benedetti et al.* [28], which considers all variability sources simultaneously.

Literature agrees that more uniformed results are obtained when similar biomechanical models are implemented. The differences in the kinematic outcomes due to different biomechanical definitions are recognised and should be taken into account for clinical decision-making and the same biomechanical model should be used for patients and normative data comparison [30].

Kadaba et al. [33] and *Flux et al.* [30] calculated the offset between the mean kinematic curves and used it to correct results variability with improved outcomes. However, this can account only for constant differences between the outcome curves, like the vertical shift found mostly on the sagittal plane [28, 30], and actual differences between models' definitions were not assessed.

1.3 Objectives

In order to overcome the aforementioned limitations and to provide repeatable and comparable kinematic outcomes, this study takes a step back in the gait analysis procedure and focuses on the core problem – the biomechanical models definitions. Therefore, the objectives of the present study are:

1. Quantify the differences between three widely adopted biomechanical models (CGM, CAST, LAMB) in terms of rotational and translational offsets between respective AFs.

2. Harmonise models with coordinate transformation (CT) and with IK. In particular, the CT harmonisations involve three transformations based on the calibration trial, the mean of the task trial and the frame-by-frame of the task trial. The dynamic transformation is included as the AL local coordinates in the TF vary with the joint motion due to the STA [9, 34]. Finally, IK harmonisation involves the same underlying model and the three biomechanical models' markersets.

3. Evaluate results' comparability.

Only joint angle kinematic data are considered, as spatio-temporal parameters present excellent consistency [28] and the kinetic outcomes are highly correlated [27] when different biomechanical models are compared. Moreover, the intrinsic accuracy of each model is not addressed as none can be considered as ground truth [3, 26, 30].

2 Methods

2.1 Protocol

Eleven healthy subjects, five women and six men, participated in this study, however, two (women) were excluded due to technical issues. The participants had no previous history of orthopaedic or neurological pathologies and no pain during walking (Table 1). All subjects gave informed consent to participate in the study, approved by the Human Research Ethics Committee of Delft University of Technology (The Netherlands). The experiment was performed at the BioMechaMotion Lab at Delft University of Technology.

Table 1: Included subjects characteristics: mean values and standard deviation (SD).

	Mean $\pm$ SD
Age [y]	28.3 $\pm$ 7.8
BMI[1] [kg/m^2]	24.5 $\pm$ 3.4
Walking speed [m/s]	3.5 $\pm$ 0.5

[1] BMI – Body Mass Index

A single marker-set (Figure 3) was created by accounting for CGM, CAST and LAMB models. The merged markerset consisted of 44 retroreflective passive markers (details in Table B.1, Appendix B). Two additional markers were placed on torso during calibration trial for OpenSim scaling, for a total of 46 markers. To increase the inter-operator reliability, one operator performed all marker placements with training and assistance of a 15 years experienced physical therapist. After markers placement, a dynamic calibration trial was recorded, which was used to train automatic identification of markers (AIM model) in Qualisys Track Manager Software (QTM, version 2020.2).

Subsequently, one calibration static trial was recorded with the subject in standing up-right position. Finally, the dynamic task consisted of barefoot, level walking at self-selected fixed speed on a treadmill for 30s and 15s. At least five gait cycles[1] were collected and five right strides were analysed for each participant based on good quality of the marker trajectories.

The 3D markers trajectories were collected using 12 tracking cameras system with sampling rate of 100Hz (Qualisys AB, Götevorg, Sweden). Prior to each experiment, the motion capture system was calibrated as follows: an L-shaped reference was placed on the treadmill to define the global laboratory coordinate system (GF); a T-shaped calibration wand (601.3mm) was used to calibrate the 3D measurement volume for 60s. The GF was defined as follows: x – backward, y – medio-lateral and z – vertical axis (Figure 3).

[1] A gait cycle starts when one foot is in contact with the floor (i.e. IC – initial contact) and ends when the same foot touches the floor in the next occasion. Considering one leg, as reference, two main phases can be distinguished in the gait cycle: stance, when the reference foot is on the ground and swing, with the reference foot in the air. For healthy subjects the stance phase is approximately 60% of the full gait cycle and the swing phase 40% [2, 5].

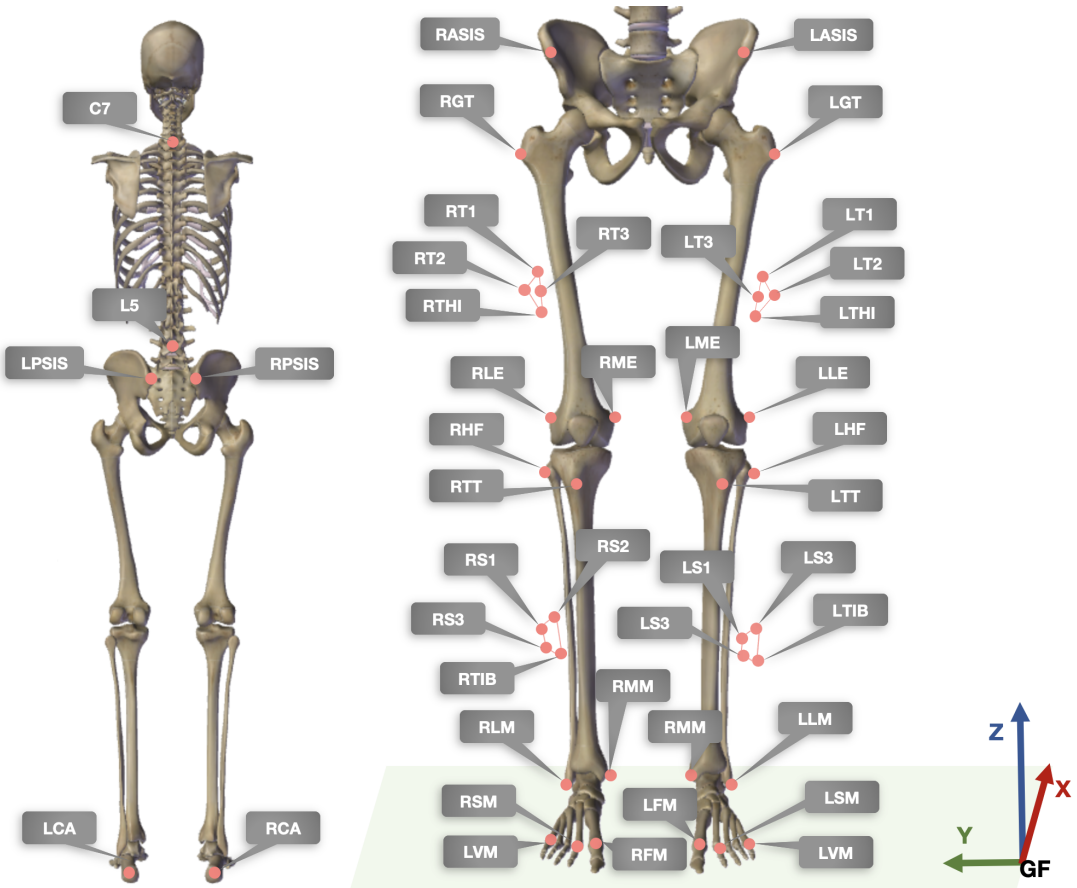

Figure 3: Merged markerset with the global coordinate system (GF). Markers connected by lines indicate that those markers are part of a plate.

2.2 Data Analysis

Markers trajectories were processed with QTM. All markers were labelled and an AIM model was created and trained to identify markers automatically in all trials. If necessary, the labelling was corrected manually. Gaps in the trajectories were filled by using polynomial gap filling. Finally, the trajectories were filtered by using moving average smoothing.

The gait cycle was identified based on the foot contact from kinematic data: minimum of the calcaneus (CA) marker's z coordinate. Gait cycles were normalised to 0-100%. Five right strides were averaged for each participant – single virtual trial, as the variability between repetitions is smaller than between biomechanical models [27], and the virtual trial was exported as C3D file. Python Btk Biomechanical ToolKit[2] was used to work with C3D files.

Kinematic data were calculated using the three biomechanical models, implemented in a custom Python (version 2.7) script, according to AFs definitions reported in Table B.2 (Appendix B). CGM was implemented as in Vicon Nexus (version 2.9) with two differences: the AFs mediolateral axes were directed to the right to allow more straightforward comparison between the models; KJC and AJC were calculated as midpoints between epicondyles and malleoli respectively, not with the chord function. CAST was implemented as in BodyMech (version 3.06.01), in which HJC is calculated according to *Leardini et al.* [35], not with the functional method as

[2] Btk Biomechanical ToolKit

proposed originally by *Cappozzo et al.* [11]. The functional joint center calculation requires the performance of a large range of motion (ROM), which may not be possible when impaired population is analysed [12, 30]. Moreover, as the purpose of this study is to assess the differences between AFs and to harmonise results, despite of biomechanical model realistic outcomes, the HJC choice is not relevant at this stage of the analysis. The HJC, calculated with both methods, is based on anatomical calibration performed during the calibration trial and its position is then reconstructed in each frame of the task trial. Thus, with both methods the problem is reduced to reconstruct a point in the dynamic trial, despite its accurate estimation. LAMB biomechanical model was based on *Rabuffetti et al.* [16].

The calibration trial ALs were also used to calculate the anthropometric measures used for the HJC regression equations: pelvis width with RASIS-LASIS markers, pelvis depth as distance between RPSIS and RASIS markers, pelvis anterior-posterior distance between RPSIS and RGT, and leg length between RASIS and RLE markers.

AFs assessment and parameters calculation were also performed in Python. AFs analysis involved rotational and translational offsets between two models (CGM-CAST, CGM-LAMB, CAST-LAMB) as function of gait cycle. The offset was obtained by, first, decomposing the ${}_{GF}T_{AF}$ in three rotations with Euler transformation (sequence of rotation: y-x-z), and three translations for two models and, secondly, by calculating the difference between the two poses. Rotations are in degrees and translations in millimeters. The offset range was calculated by considering the curve peaks (maximum and minimum), and the deviation range (SD maximum and minimum).

Fifteen clinically relevant kinematic parameters for pelvis, thigh, shank and foot were calculated, as in *Flux et al.* [30] and were calculated for all kinematic curves (Table 5).

As for OpenSim IK analysis, the virtual trial was exported to MATLAB (r2020, The MathWorks, Inc., Natick USA) and prepared for the OpenSim software input format (trc) by using the OpenSim MATLAB script (osimC3D), which transforms data from the motion capture GF to OpenSim GF. The procedure followed OpenSim Best Practices[3] and it is described details in section 2.3.2.

2.3 Models Harmonisation

The *harmonisation* process aims to produce consistent and comparable results provided by the biomechanical models. Transformations from CAST to CGM, from LAMB to CGM and from LAMB to CAST were considered for the CT. The CT harmonisations included three transformations types based on the calibration trial, the mean of the task trial and the frame-by-frame of the task trial. The IK harmonisation consisted in OpenSim IK fitting with the three models' markersets and same underlying OpenSim model with the corresponding virtual markersets.

In order to clarify the nomenclature: the results calculated directly by the biomechanical models (CGM, CAST, LAMB) are referred as *native*, while the transformation from one model to another is referred as *harmonised* (e.g. transformation from CAST to CGM is referred as CGM harmonised from CAST). Also the IK results are referred as OpenSim/IK harmonised.

[3] OpenSim – Best Practices

2.3.1 Coordinate Transformation

The CT harmonisation transforms AFs from one model to another by calculating the *universal*[4] transformation matrix (uT) for the subject involved in the harmonisation process. uT provides the transformation from one model – *native*, to another model – *target*, and is calculated for each body segment's AF. As the biomechanical model's definitions (Table B.2, Appendix A) provide the transformation matrix from GF to AF, ${}_{GF}T_{AF}$, the uT is calculated according to eq. 1:

$$ {}_{AF(native)}uT_{AF(target)} = {}_{GF}\ T^{-1}_{AF(native)} * {}_{GF}\ T_{AF(target)} \tag{1} $$

The CT harmonisation was performed for three different calculations of uT: (1) calculated during the static calibration trial: uT_s; (2) as mean of the task trial by considering the normalised gait cycle: uT_m; (3) as dynamic frame-by-frame transformation, by considering each frame of the normalised gait cycle: $uT_{fbf}(f)$.

To calculate uT, leave-one-out strategy was adopted: 8 subjects were used interchangeably to calculate the uT for the 9^{th} subject. The subject involved in the harmonisation process was not included in the uT calculation in order to avoid biased results.

The uT was then used to transform the AFs, for each segment and for each frame, according to eq. 2:

$$ {}_{GF}Th_{AF(target)}(f) = {}_{GF}\ T_{AF(native)}(f) *_{AF(native)}\ uT_{AF(target)} \tag{2} $$

where ${}_{GF}Th_{AF}$ is the harmonised transformation matrix from GF to AF.

The uT_s and uT_m are calculated only once, therefore, the uT is constant across the gait cycle (the same matrix is used to transform each frame), while $uT_{fbf}(f)$ differs for each frame. The three harmonisation are further referred as static, mean and frame-by-frame harmonisations.

Finally, the ${}_{GF}Th_{AF}$ of distal and proximal segments were used to calculate joint angles with the angles decomposition convention according to the target model.

2.3.2 Inverse Kinematics

For the IK approach, OpenSim (version 4.2) [22] was used, as it is an open-source and mostly used musculoskeletal model software. The model used in this analysis is Gait2354 [25] with 3-1-1 degrees of freedom on hip, knee and ankle respectively. According to *Roelker et al.* [24], Gait2392 is accurate enough to assess healthy walking. Gait2392 and Gait2354 have the same number of DoFs and differ in number of muscles and, as this study is not interested in muscular analysis, Gait2354 was used for IK analysis. Moreover, by using the same underlying model and by constraining the model's DoFs, errors related to STA and inconsistencies due to markers placement are reduced [30].

The OpenSim harmonisation procedure involved the implementation of respective virtual markerset on the OpenSim lower limb model [36] in the corresponding locations as the ALs and

[4] In a real case scenario one laboratory implements only one model, thus, a transformation matrix from one model into another should be available in literature in order to obtained harmonised results.

TMs of the biomechanical models. For the scaling process, the calibration trial was used with all markers available for the model in analysis. For this procedure, two additional markers were implemented to scale the torso segment (Table B.1, Appendix B). The segments scaling involved scale factors based on ALs position as specified in Table B.3. The same scaling was applied to all biomechanical models. The scaling procedure, first, creates a subject-specific model and, then, it adjusts virtual markers according to recorded data. The subject-specific model with the associated markerset was used to solve the IK. The IK analysis was performed by tracking only TMs corresponding to each biomechanical model marker-set separately. The virtual trial for each participant was used for the OpenSim IK procedure. The weights used in scaling are adapted from *Falisse et al.* [37] and reported in Table B.4 (Appendix B), the weight in IK were uniform and equal to 1 [37].

Results from OpenSim were exported and analysed in Python. Knee flexion/extension joint angle was reversed.

2.4 Statistics

Leave-one-out cross-validation strategy was used to calculate the uT, as part of the data set (i.e. 8 on 9 subjects) was needed to build the harmonisation universal matrices for each segment, which were applied to harmonise the 9^{th} subject and to validate the results.

Statistical analysis was performed to quantify the differences between AFs, kinematic curves and parameters, and to test whether this difference is statistically significant.

Joint kinematic differences between biomechanical models, between biomechanical models and harmonised joint angles results (both CT and IK) were evaluated with paired t-tests by using Statistical Parametric Mapping (SPM 1D on MATLAB, version 0.4.3). The Holm correction was implemented[5] to maintain the probability of type 2 error at 5%, as in *Flux et al.* [30]. SPM allows to identify statistically significant differences locally along the curve.

Kinematic parameters were calculated in Python, exported and analysed in RStudio (version 1.3.1073). Data normality was assumed and not tested, as the sample size is not big enough to verify normality reliably [38]. Paired t-tests with Holm correction were performed to verify the difference significance.

For all tests, the significance level was set to 0.05.

Root mean square errors (RMSEs) were calculated to quantify the difference (as effect size) between two curves. RMSEs for kinematic curves were calculated for each subject for each kinematic curve, then averaged between subjects.

As suggested by *McGinley et al.* [26] and *Wilken et al.* [39], differences higher than 5° are clinically relevant. Thus, a minimal clinically important difference (MCID) of 5° is considered to detect clinically significant differences between kinematic curves and parameters.

[5] David Groppe (2020). Bonferroni-Holm Correction for Multiple Comparisons, MATLAB Central File Exchange. Retrieved September 12, 2020

3 Results

Due to the current Covid-19 pandemic, experiments were postponed. Therefore, data from *Ferrari et al.* [27] were initially used to implement the models and the harmonisation process. In this section, only data from our experiment are presented.

Firstly, results from native models are described in section 3.1, secondly, the differences between AFs are quantified in section 3.2. Finally, the harmonised results are presented in section 3.3 for the CT, and in 3.4 for the IK. All the results are described in the text, however, the graphical representation reported here focuses on CGM-CAST comparison and harmonisation from CAST to CGM, while the remaining figures can be found in the Appendix C.

3.1 Native Models Results

Kinematic curves for the three native models are in Figure 4, SPM t-tests for CGM-CAST comparison are in Figure 5, while in Appendix C there are results for CGM-LAMB and CAST-LAMB (Figures C.1 and C.2). RMSEs between the three native models are reported in Figure 6. The kinematic parameters are in Table 5, while the statistical comparison between native models' kinematic parameters are in Table 2.

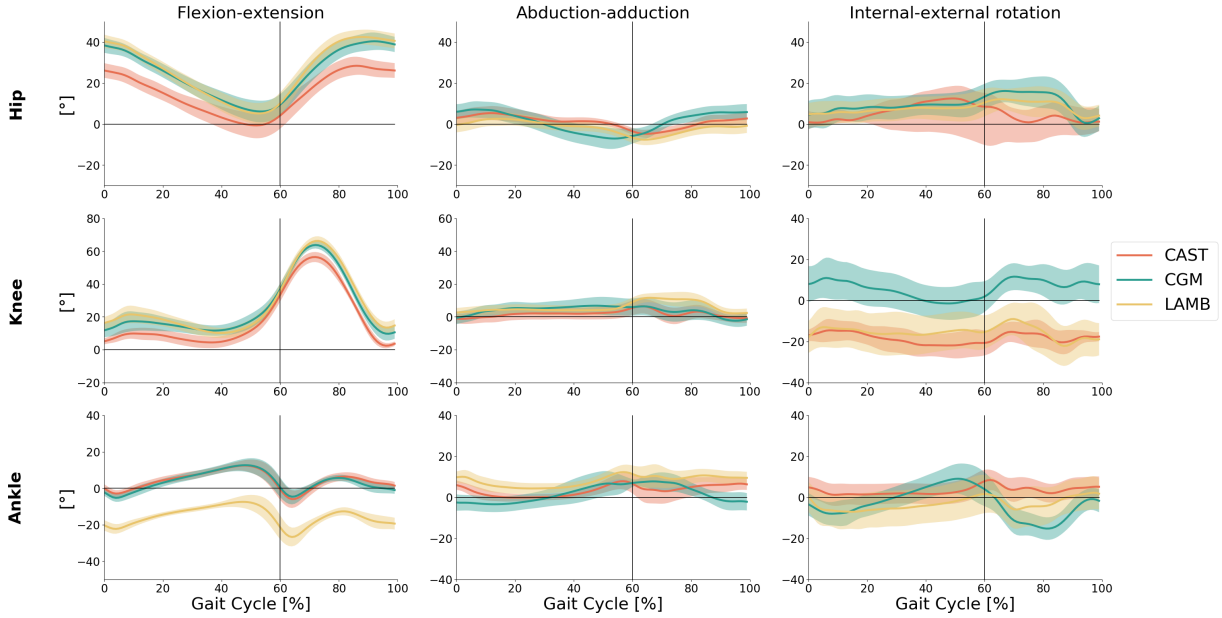

Figure 4: Kinematic curves for sagittal (flexion/extension), frontal (abduction/adduction) and transverse (internal/external rotation) planes angles for hip, knee and ankle from the three native models: CGM, CAST, LAMB. The gait cycle was normalised 0-100%. The vertical line indicates toe-off (i.e. stance and swing phases).

SPM results show significant differences for most of the curves, with the exception of knee abduction-adduction for CGM-LAMB and ankle internal-external rotation for CAST-LAMB.

RMSEs provide differences higher than 5° (MCID) for hip flexion/extension for CGM-CAST and CAST-LAMB comparisons, for knee flexion/extension for CGM-CAST and CAST-LAMB, knee

internal/external rotation for CGM-CAST and CGM-LAMB. All ankle angles RMSEs exceed MCID, except plantar-/dorsi-flexion for CGM-CAST. The differences on sagittal plane consist in vertical shift, while on the other planes even opposite pattern is observed.

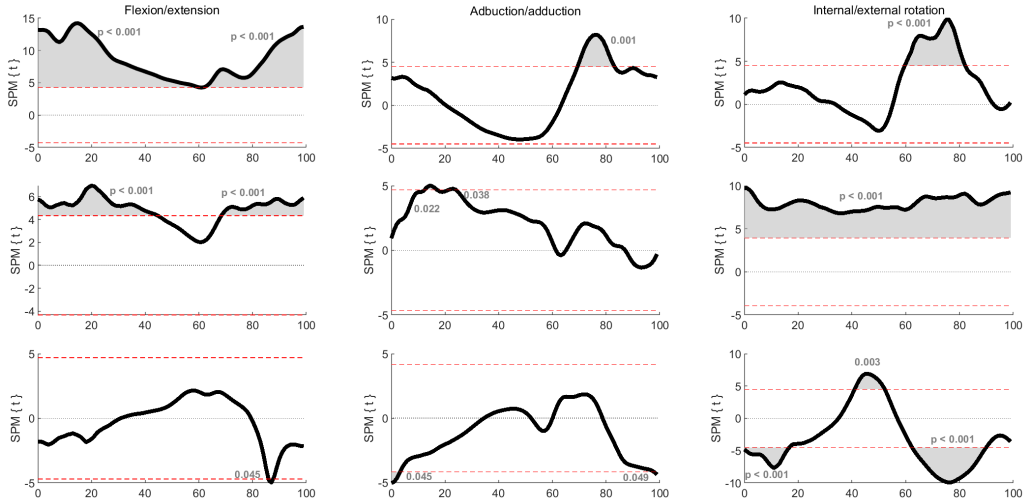

Figure 5: Paired t-test results for CAST-CGM comparison, obtained from SPM, as function of the normalised gait cycle. Red dash horizontal lines indicate a threshold where there is significant difference, grey area represents significant difference with bigger grey area being associated with lower p-value.

Also most of the kinematic parameters exceed MCID. Differences higher than MCID for CGM-CAST are: minimum hip flexion (6.8°), peak hip endorotation (5.3°), peak knee flexion swing (7.3°), and stance (6.7°), knee flexion at IC (6.7°); for CGM-LAMB: peak ankle dorsal stance (19.9°) and swing (19.2°), peak plantar push-off (21.7°); for CAST-LAMB: ROM hip flexion (7.9°), minimum hip flexion (5.1°), peak hip exorotation (5.2°), peak knee flexion swing (9.8°) and stance (6.7°), knee flexion at IC (11.2°), peak ankle dorsal stance (19.7°) and swing (19.6°) and peak plantar push-off (20.7°).

Table 2: Kinematic parameters t-test outcome for native models.

	CGM-CAST	CGM-LAMB	CAST-LAMB
ROM[1] hip flexion	**0.012**	**0.001**	**<0.001**
Minimum hip flexion	**<0.001**	**0.016**	**0.002**
Peak hip abduction swing	**0.160**	**0.036**	**<0.001**
Peak hip exorotation	0.148	0.119	**0.002**
Peak hip endorotation	**0.013**	**<0.001**	0.634
ROM knee flexion	0.746	0.323	0.121
Peak knee flexion swing	**<0.001**	0.099	**<0.001**
Peak knee extension stance	**<0.001**	0.980	**<0.001**
Knee flexion at IC[2]	**<0.001**	**0.004**	**<0.001**
Time to peak knee flexion	0.195	0.169	**0.023**
ROM knee adduction	**0.012**	0.139	0.211
Peak ankle dorsal stance	0.835	**<0.001**	**<0.001**
Peak ankle dorsal swing	0.418	**<0.001**	**<0.001**
Peak plantar push-off	0.226	**<0.001**	**<0.001**
Mean foot progression	**<0.001**	**0.007**	**0.020**

Notes: [1]ROM – range of motion; [2]IC – initial contact;
Underlined results exceed MCID ($5°$).

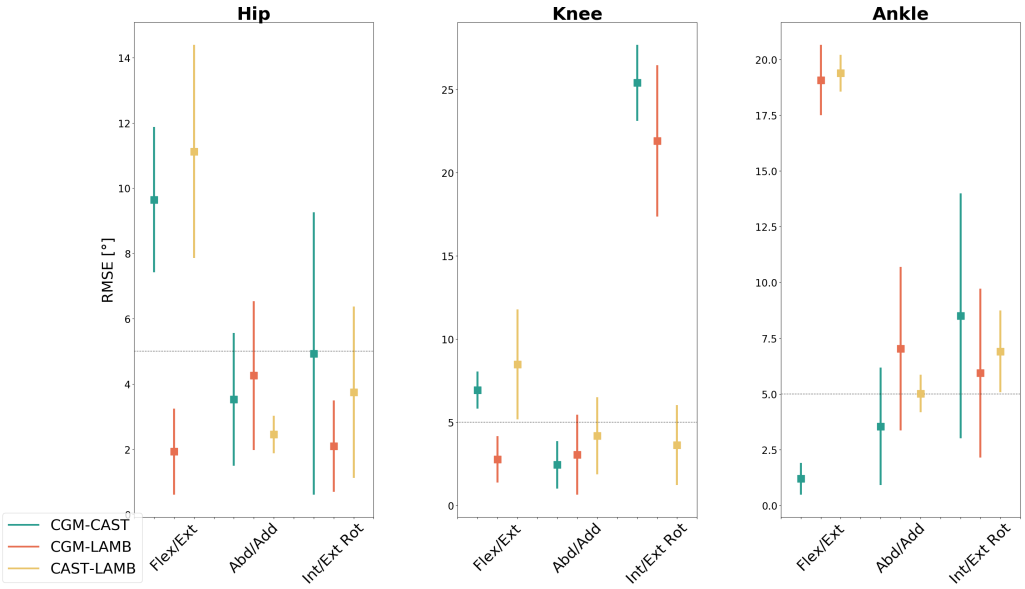

Figure 6: RMSE between each combination of the native biomechanical models. The horizontal black line indicates MCID (5°).

3.2 Anatomical Frames Analysis

The rotational and translational offsets as function of the gait cycle between CGM-CAST are represented in Figure 7, while between the other models in Appendix C: Figures C.9 and C.10. The offset range between all coupled native models' definitions is reported in Table 3.

A qualitative representation of two models AFs can be found in Appendix C. In particular, CGM and CAST AFs for one participant and for each segment during calibration trial are in Figure C.3, while the AFs reported as mean across the gait cycle are in Figure C.4, AFs of CGM and LAMB are in Figures C.5 and C.6 and AFs of CAST and LAMB in Figures C.7 and C.8.

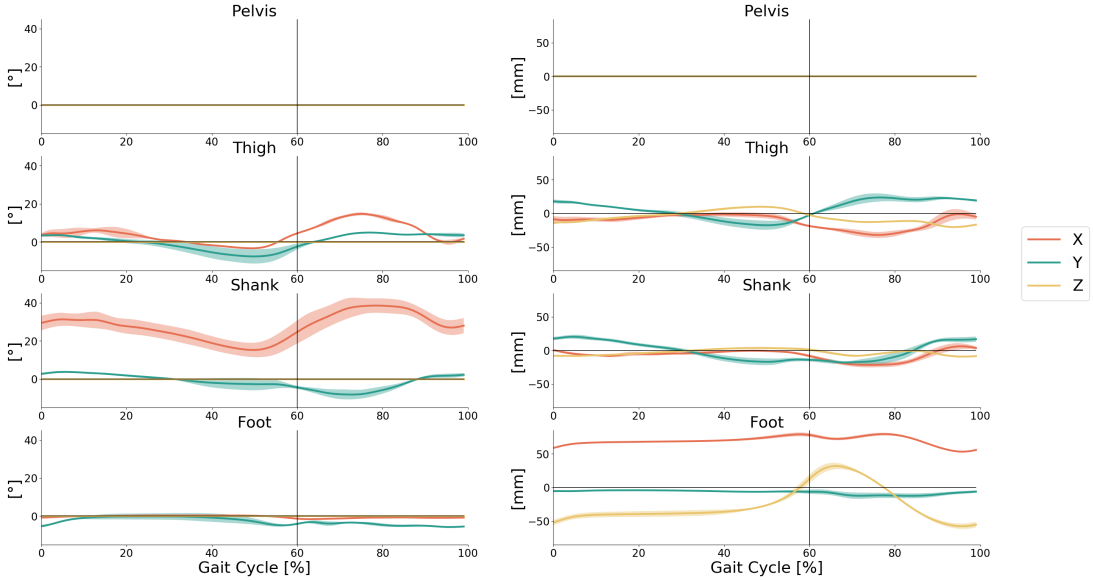

Figure 7: Rotational and translational offsets decomposed on the three axes between CGM and CAST AFs for each segment.

Table 3: Rotational and translational offset range between AFs definitions: [max curve; min curve], [max SD; min SD].

	Rotation [°]			Translation [mm]		
	X	Y	Z	X	Y	Z
CGM-CAST						
Pelvis	[0.0;0.0][0.0;0.0]	[0.0;0.0][0.0;0.0]	[0.0;0.0][0.0;0.0]	[0.0;0.0][0.0;0.0]	[0.0;0.0][0.0;0.0]	[0.0;0.0][0.0;0.0]
Thigh	[-5.2;-13.4][1.7;0.0]	[5.0;-7.4][3.8;0.0]	[14.8;-3.3][2.7;0.0]	[-1.1;-32.1][8.4;1.5]	[23.3;-17.7][6.8;0.1]	[9.9;-20.4][2.1;0.0]
Shank	[-0.2;-5.8][1.7;0.0]	[3.7;-8.2][3.3;0.0]	[38.5;15.2][6.4;3.3]	[6.1;-21.6][5.4;0.1]	[20.3;-18.2][6.4;1.7]	[3.7;-9.1][2.1;0.0]
Foot	[-1.1;-3.1][0.9;0.0]	[-0.2;-5.8][2.2;0.0]	[0.3;-1.6][0.3;0.0]	[79.5;53.4][2.9;0.0]	[-4.1;-12.4][4.7;0.6]	[32.0;-57.6][6.6;0.1]
CGM-LAMB						
Pelvis	[0.0;0.0][0.0;0.0]	[0.0;0.0][0.0;0.0]	[-0.8;-0.8][0.8;0.2]	[0.0;0.0][0.0;0.0]	[0.0;0.0][0.0;0.0]	[0.0;0.0][0.0;0.0]
Thigh	[4.0;-1.0][0.8;0.0]	[6.9;-4.6][3.1;0.0]	[4.3;-3.0][2.1;0.0]	[2.4;-17.2][2.3;0.0]	[23.1;-16.3][8.0;0.2]	[3.9;-5.5][1.6;0.0]
Shank	[2.3;-2.7][1.3;0.0]	[4.0;-8.3][4.2;0.2]	[34.3;12.6][2.6;0.0]	[3.9;-15.9][5.2;0.0]	[22.2;-17.9][7.7;1.9]	[4.4;-8.7][1.4;0.0]
Foot	[-17.0;-20.8][2.0;0.2]	[-6.5;-14.5][1.5;0.0]	[2.6;-1.7][1.5;0.0]	[1.0;-0.8][1.0;0.0]	[0.7;-3.1][1.6;0.4]	[-0.2;-1.5][0.7;0.0]
CAST-LAMB						
Pelvis	[0.0;0.0][0.0;0.0]	[0.0;0.0][0.0;0.0]	[-0.8;-0.8][-0.8;0.2]	[0.0;0.0][0.0;0.0]	[0.0;0.0][0.0;0.0]	[0.0;0.0][0.0;0.0]
Thigh	[15.0;5.3][2.0;0.0]	[3.8;0.5][0.8;0.0]	[4.1;-10.6][2.5;0.1]	[15.5;-4.7][6.3;0.4]	[4.9;-2.0][3.2;0.1]	[15.2;-6.0][2.0;0.0]
Shank	[3.6;1.5][0.6;0.0]	[1.1;-0.2][1.7;0.6]	[-1.5;-7.9][5.0;2.0]	[10.0;-4.8][2.3;0.0]	[2.9;-1.3][1.4;0.0]	[8.5;-1.0][2.8;0.0]
Foot	[-16.0;-17.8][1.5;0.8]	[-6.3;-10.0][1.1;0.1]	[2.3;-0.3][1.3;0.0]	[-54.2;-78.7][2.6;0.0]	[12.2;0.9][3.6;0.0]	[57.4;-33.5][7.2;0.0]

The AFs analysis shows the differences between biomechanical models definitions, in terms of axes rotations and origin translations. Pelvis AFs definitions are the most similar between all models and the origins are equal between all models (i.e. midpoint between RASIS and ASIS markers). Thigh and shank AFs origins also share the same definitions (i.e. KJC and AJC calculated as midpoints between epicondyles and malleoli, respectively, in each model). However, as the calibration trial AFs are consistent with the definitions, the task trial AFs figures show shifted origins and rotated axes. The only real difference between origins is in the foot AFs origins: for CGM and LAMB, the origin is located in the AJC, while for CAST in the CA marker.

The variability in the definitions across the gait cycle is shown in the offset figures (7, C.9 and C.10) and quantified and reported as range in Table 3. The range represents the curve's peaks and the SD maximum and minimum along the curve.

The rotational offset reaches highest variability between the shank AFs Z axes for CGM-CAST (23.3°) and for CGM-LAMB (21.7°); between thigh AFs X axes for CAST-LAMB (20.3°); shank AFs Z axes for CAST-LAMB (14.7°); and shank AFs Y axes for CGM-CAST (11.9°) and CGM-LAMB (12.3°).

The translational offset is high along the thigh Y axis for CGM-CAST (41.0mm) and CGM-LAMB (39.4mm); along the thigh Z axis for CGM-CAST (30.3mm); along shank X axis for CGM-CAST (27.7mm) and CGM-LAMB (19.8mm); along shank Y axis for CGM-CAST (38.5mm) and CGM-LAMB (40.1mm). The translational offset between foot AFs are explained by the different implemented origins. Although CGM and LAMB share the same foot origin (AJC), a maximum difference of 3.8mm along the Y axis is found.

Moreover, the variability between models' definitions is higher than the variability between subjects (represented by the SD). Maximum rotational variability between subjects is 3.8° for CGM-CAST between thigh AFs Y axes, and maximum translational variability is 7.8mm for CGM-LAMB along thigh Y axis.

3.3 Coordinate Transformation Harmonisation

The harmonised results, for CAST to CGM transformation, are represented in Figure 8 together with native CGM outcomes. The harmonised results include the three harmonisations: frame-by-frame, mean and static. The corresponding SPM statistics results between native CGM and CGM frame-by frame harmonised from CAST are in Figure 9, between native CGM and CGM mean harmonised are in Figure 10, while the static harmonisation statistics in Figure 11 and RMSE in Figure 12.

The kinematic curves for LAMB to CGM and LAMB to CAST harmonisations are reported in the Appendix C, Figures C.11 and C.12. The corresponding statistical SPM t-tests are in Figures C.15-C.20 and RMSE are in Figures C.13 and C.14 (Appendix C).

The kinematic parameters for all models are in Table 5, and harmonisation statistics in Table 4.

Frame-by-frame harmonisation shows comparable results, as confirmed by the SPM, with no statistical difference between harmonised and native kinematics for each harmonisation (from CAST to CGM, from LAMB to CGM and from LAMB to CAST), but also by RMSE and kinematic

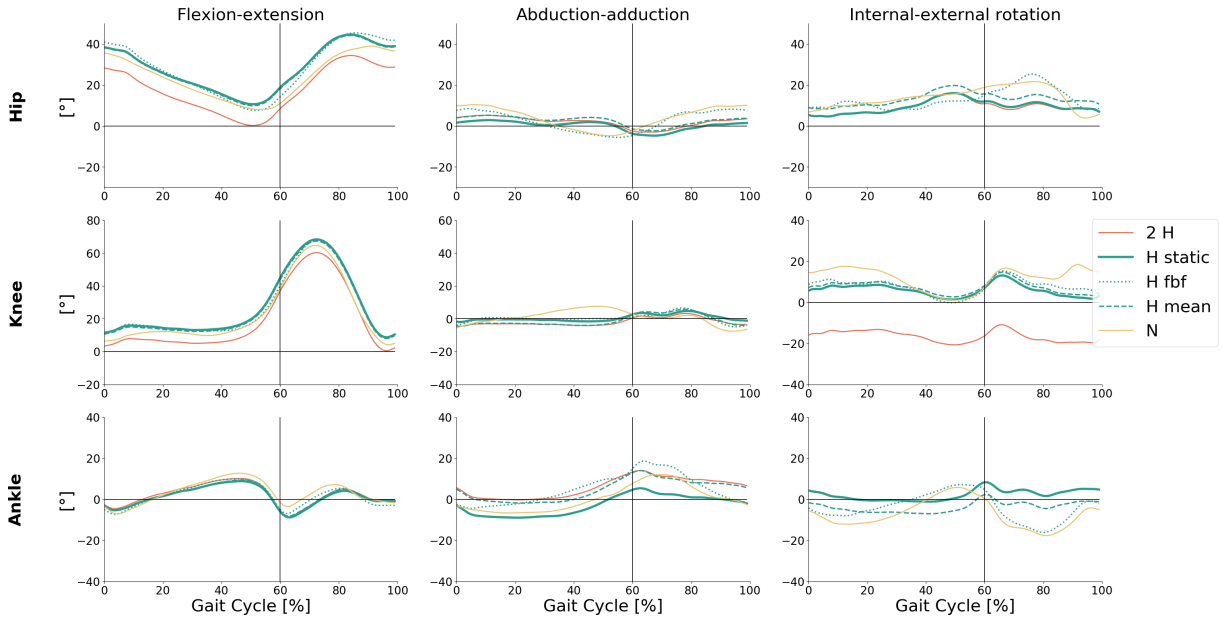

Figure 8: CT harmonised kinematic curves for the transformation from CAST to CGM for a typical subject. The red solid line indicates the CAST native (2H – to harmonise) results; the solid yellow line represents the CGM native curves (N – native/target); the blue line are all harmonisations (H): solid – static, dot – frame-by-frame and dashed – mean.

parameters differences being below MCID.

CAST to CGM harmonisation with uT calculated as mean between frames shows statistically significant difference for hip and ankle internal-external rotation. Only ankle internal-external rotation RMSE exceeds MCID. All kinematic parameters are below MCID.

Static CAST to CGM harmonisation shows a statistically significant differences for hip and ankle on frontal and transverse planes, with RMSE higher than MCID only for the ankle joint angles on out-of-sagittal planes. Only hip flexion ROM exceeds MCID (5.1°), however, RMSE on the entire curve is below MCID.

LAMB to CGM static harmonisation reports RMSE for ankle internal-external rotation being higher than MCID.

Clinically significant difference for LAMB to CAST mean harmonisation is found for hip flexion ROM (7.9°), minimum hip flexion (5.0°), while for the static harmonisation for hip flexion ROM (7.9°).

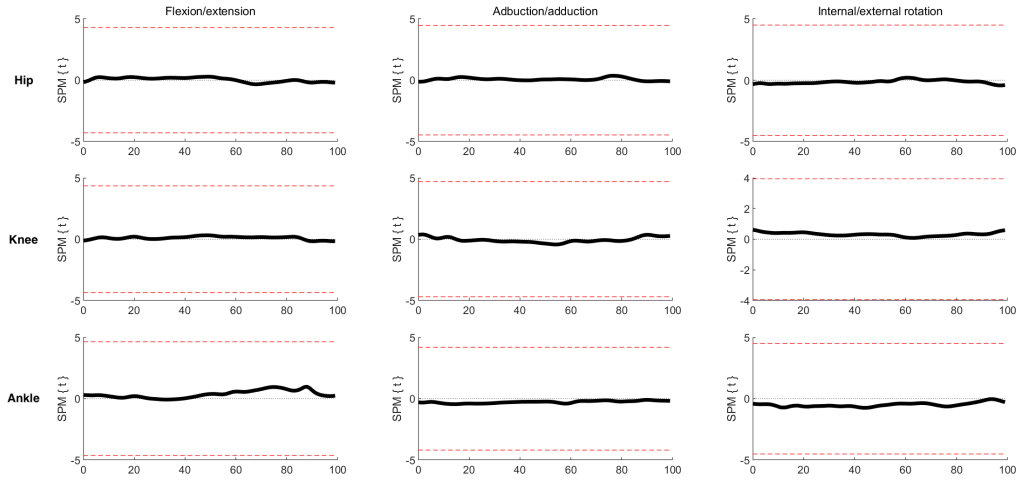

Figure 9: SPM t-test t-values for CGM harmonised from CAST with frame-by-frame CT.

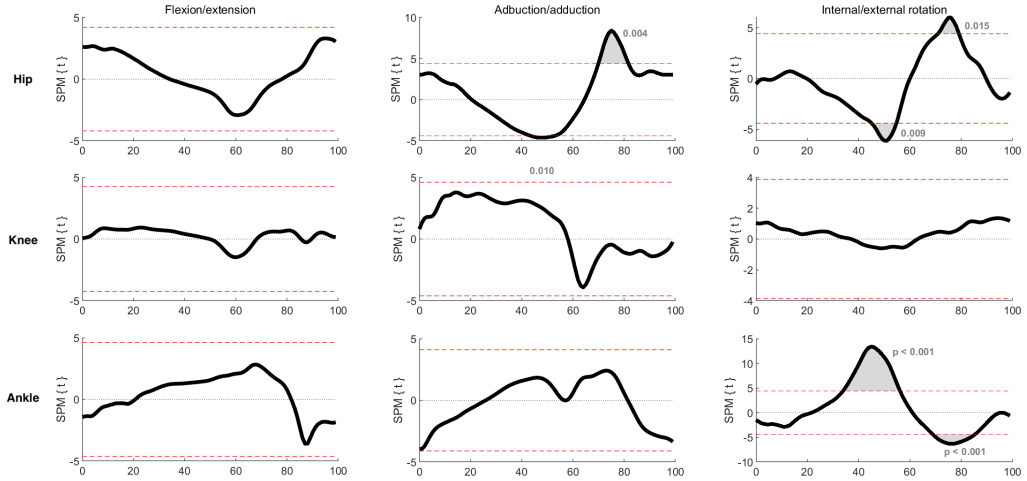

Figure 10: SPM t-test t-values for CGM harmonised from CAST with mean CT.

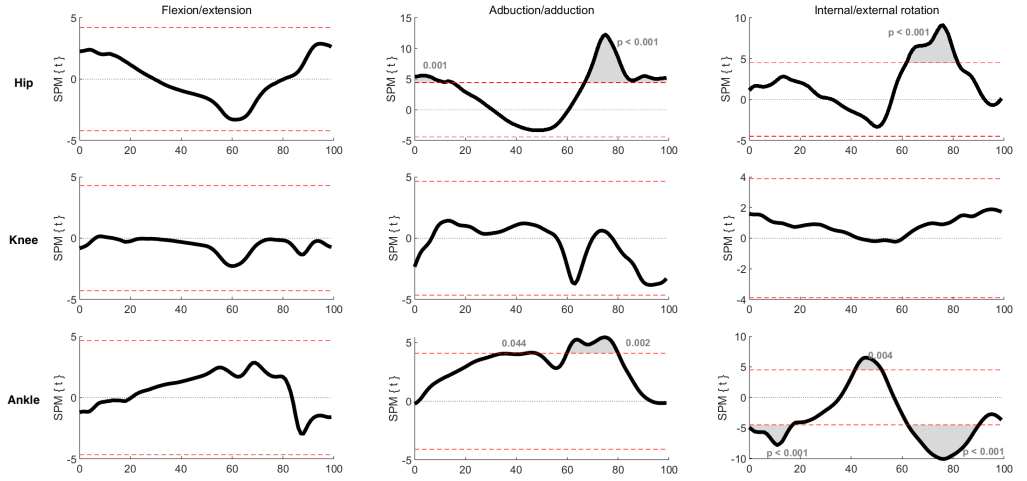

Figure 11: SPM t-test t-values for CGM harmonised from CAST with static CT.

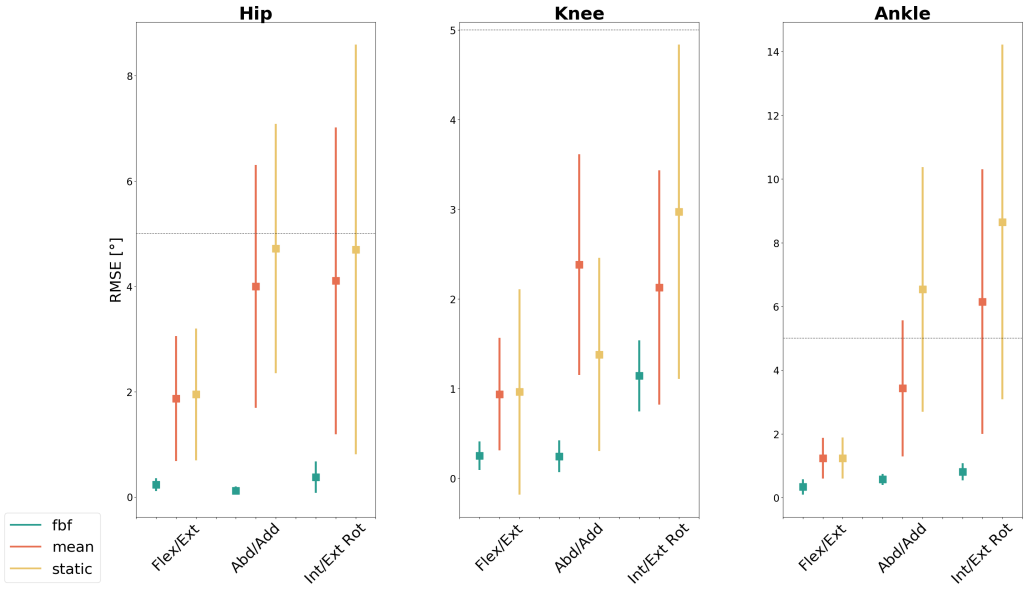

Figure 12: RMSE between native CGM and CGM harmonised from CAST for the three harmonisation types (fbf – frame-by-frame, mean and static).

Table 4: Kinematic parameters t-test outcome for each harmonisation.

	CGM-CAST2CGM[4]			CGM-LAMB2CGM			CAST-LAMB2CAST		
	fbf[3]	mean	static	fbf	mean	static	fbf	mean	static
ROM[1] hip flexion	0.782	**0.013**	**0.010**	0.947	**0.010**	**0.011**	0.797	**<0.001**	**<0.001**
Minimum hip flexion	0.940	0.114	0.053	0.998	**<0.001**	**0.020**	0.926	**0.011**	**0.027**
Peak hip abduction swing	0.742	0.112	0.223	0.799	0.329	0.059	0.894	0.132	0.071
Peak hip exorotation	0.979	0.530	0.242	0.522	**0.016**	0.053	0.248	**0.032**	**<0.001**
Peak hip endorotation	0.608	0.620	**0.020**	0.547	**0.003**	**<0.001**	0.755	0.149	0.962
ROM knee flexion	0.694	0.704	0.763	0.763	0.579	0.323	0.832	0.144	0.194
Peak knee flexion swing	0.896	0.616	0.752	0.785	0.566	**0.010**	0.963	0.445	0.331
Peak knee extension stance	0.833	0.993	0.446	0.838	0.237	0.980	0.856	0.294	0.472
Knee flexion at IC[2]	0.862	0.979	0.348	0.937	0.033	**0.004**	0.902	0.078	**0.038**
Time to peak knee flexion	0.347	0.195	0.104	0.729	0.169	0.169	1.000	**0.023**	**0.023**
ROM knee adduction	0.273	0.144	**0.012**	0.115	0.792	0.139	0.308	0.435	**0.068**
Peak ankle dorsal stance	0.742	0.399	0.266	0.842	0.306	0.069	0.929	0.785	0.632
Peak ankle dorsal swing	0.833	0.825	0.522	0.743	0.969	0.178	0.692	0.851	0.838
Peak plantar push-off	0.921	0.247	0.222	0.944	0.050	**0.007**	0.967	0.407	0.439
Mean foot progression	0.921	**0.016**	**0.013**	0.464	0.053	0.051	0.535	0.498	0.577

Notes: [1]ROM – range of motion; [2]IC – initial contact; [3]fbf – frame-by-frame; [4]CGM-CAST2CGM – CGM native compared to CGM harmonised from CAST (i.e. transformation from CAST to CGM);
Underlined results exceed MCID ($5°$).

Table 5: Kinematic parameters for native and CT harmonised results (mean [°] ± SD) for native models and CT harmonisations.

	CGM	CAST	LAMB	CAST2CGM			LAMB2CGM			LAMB2CAST		
				fbf[3]	mean	static	fbf	mean	static	fbf	mean	static
ROM hip flexion	34.5±4.3	29.7±3.9	37.6±3.2	35.0±5.1	29.8±3.9	29.4±3.9	34.4±4.0	37.6±3.2	37.6±3.2	29.4±2.8	37.6±3.1	37.6±3.2
Minimum hip flexion	6.0±5.3	-0.8±6.2	5.1±5.1	5.9±7.1	8.4±6.4	9.2±6.6	6.0±5.2	3.8±5.1	5.1±5.1	-0.7±5.1	-5.8±5.1	-4.8±5.0
Peak hip abduction swing	-6.0±3.6	-4.9±2.1	-7.7±2.6	-5.7±2.0	-4.5±2.4	-7.1±2.5	-5.8±2.4	-5.3±2.5	-7.5±2.7	-5.0±2.6	-6.1±2.6	-6.3±2.5
Peak hip exorotation	-0.3±6.5	-3.4±6.4	1.8±6.1	-0.4±7.0	1.0±6.0	-2.7±6.0	0.4±5.7	3.6±6.2	2.4±6.1	-1.6±6.7	-0.6±6.4	2.0±6.3
Peak hip endorotation	18.4±5.0	13.1±5.4	13.9±5.3	19.1±5.5	17.5±5.3	13.7±5.3	17.9±5.6	15.7±5.3	14.6±5.4	12.8±5.9	10.5±5.6	13.2±5.5
ROM knee flexion	55.5±3.7	55.1±2.3	56.9±2.6	55.0±2.6	55.0±2.3	55.1±2.4	55.2±3.0	56.3±2.7	56.9±2.6	55.2±2.8	56.8±2.6	56.6±2.6
Peak knee flexion swing	63.9±2.2	56.6±3.1	66.4±2.9	63.7±3.1	63.2±3.3	64.4±3.4	63.6±3.1	64.4±2.9	66.4±2.9	56.5±3.1	57.9±3.2	58.3±3.0
Peak knee extension stance	10.1±3.2	3.4±2.7	10.1±3.1	10.4±2.8	10.1±2.8	11.2±2.8	10.2±2.9	8.7±3.1	10.1±3.1	3.1±3.4	1.8±3.4	2.3±3.4
Knee flexion at IC	11.7±4.3	5.0±1.8	16.2±3.6	11.9±1.6	11.8±1.7	12.8±2.0	11.8±3.9	14.8±3.6	16.2±3.6	4.9±3.9	7.8±4.0	8.4±3.9
Time to peak knee flexion	72.0±0.8	71.7±0.7	72.4±0.7	72.2±0.9	71.7±0.7	71.6±0.8	71.9±1.0	72.4±0.7	72.4±0.7	71.7±1.1	72.4±0.7	72.4±0.7
ROM knee adduction	13.1±3.9	9.7±3.2	11.0±2.6	11.9±2.1	11.4±3.6	9.3±2.9	10.8±1.4	12.7±2.9	11.0±2.6	8.8±2.2	10.5±2.7	11.9±2.9
Peak ankle dorsal stance	13.1±3.3	12.9±2.7	-6.8±3.0	13.4±3.0	12.4±2.8	11.9±2.7	13.3±3.2	12.1±3.0	11.0±2.9	12.8±3.1	12.7±2.9	12.5±3.1
Peak ankle dorsal swing	6.7±1.6	7.1±2.0	-12.5±2.1	6.8±2.2	6.8±2.2	6.3±2.3	6.3±2.2	6.6±1.9	5.4±1.9	6.7±1.9	6.9±1.9	6.9±1.9
Peak plantar push-off	2.6±5.6	1.6±5.9	-19.1±6.8	2.7±5.9	1.6±5.8	1.4±5.4	2.7±6.2	0.6±6.3	-0.4±5.8	-6.5±5.0	0.5±6.5	0.6±6.6
Mean foot progression	6.0±2.9	6.6±2.8	7.9±2.0	6.0±2.8	6.3±2.8	6.3±2.8	6.1±3.1	6.4±3.0	6.5±3.1	6.7±3.1	6.7±3.1	6.7±3.1

Notes: [1]ROM – range of motion; IC – initial contact; fbf – frame-by-frame.

3.4 Inverse Kinematics Harmonisation

OpenSim kinematic curves for a typical subject are in Figure 13, SPM between CGM and CAST in Figure 14, while SPM t-test between CGM and LAMB and between CAST and LAMB are in Figures C.21 and C.22, respectively (Appendix C). RMSE for all IK results are in Figure 15. Kinematic parameters with corresponding p-values from the paired t-tests are in Table 6.

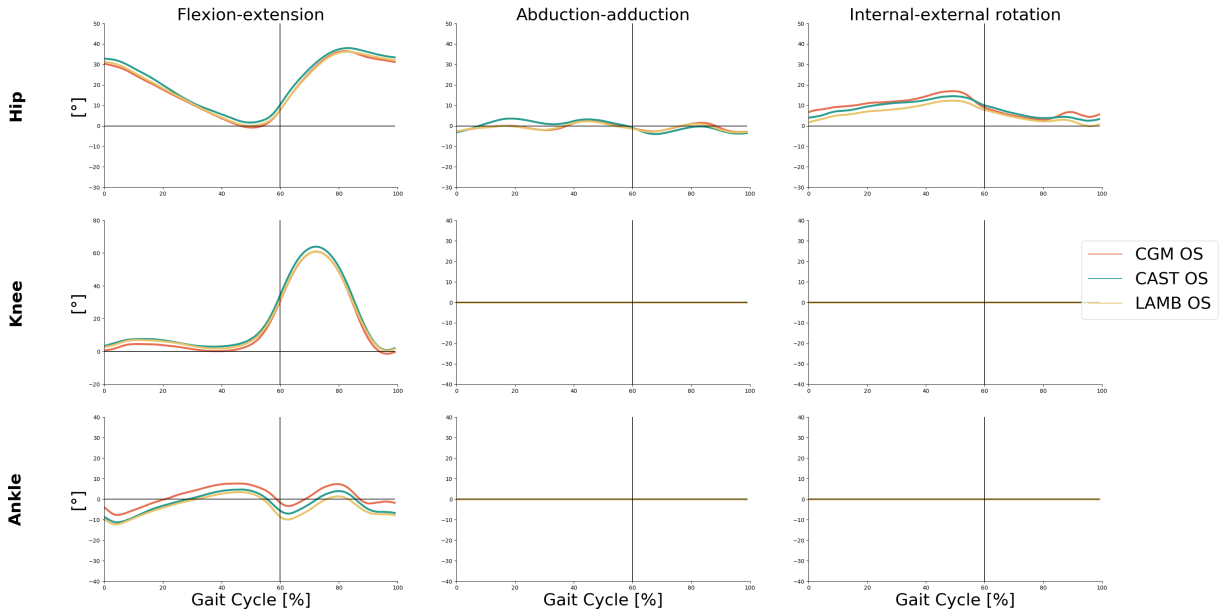

Figure 13: Kinematic curves from OpenSim IK for a typical subject for the three biomechanical models' markersets.

OpenSim scaling RMSE was 0.8±0.2cm and maximum error was 1.2±0.4cm, close to OpenSim recommendations (1cm and 2cm, respectively). IK RMSE was 1.1cm for CGM, 1.1cm for CAST and 1.2cm for LAMB, and maximum error was 2.2cm for CGM, 2.4cm for CAST and 2.6cm for LAMB, also in accordance with OpenSim Best Practices (2cm and 4cm, respectively).

OpenSim IK results are comparable when TMs from each biomechanical model are implemented as virtual markers and no opposite patterns are observed. SPM t-tests results show statistically significant difference for most of the CGM-CAST and CAST-LAMB curves, in particular during the swing phase. Only ankle flexion-extension RMSE for CGM-LAMB comparison exceeds MCID for some subjects. Only two kinematic parameters exceed MCID between CGM and LAMB markersets: peak ankle dorsal swing (6.2°) and peak plantar flexion at push-off (7.1°).

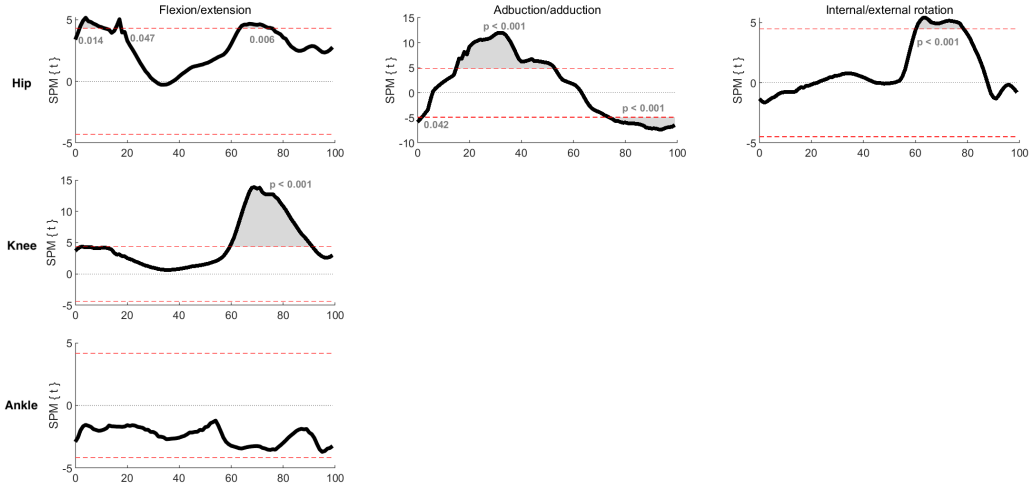

Figure 14: SPM t-test between IK CAST and CGM.

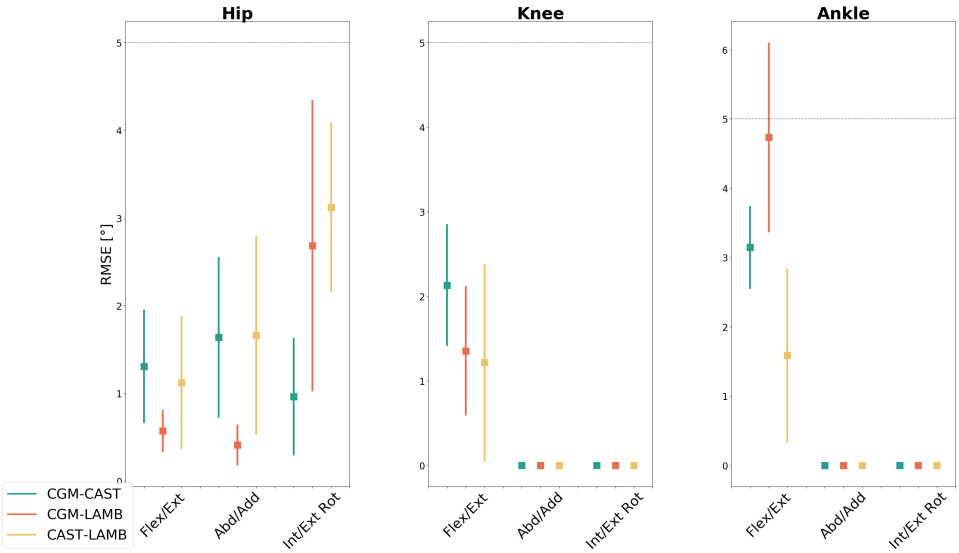

Figure 15: Kinematic curves from OpenSim IK for all subjects.

Table 6: Kinematic parameters (mean [°] ± SD) and t-test for IK harmonised results.

	Kinematic parameters			P-values from paired t-tests		
	CGM	CAST	LAMB	CGM-CAST	CGM-LAMB	CAST-LAMB
ROM[1] hip flexion	38.7±3.9	38.7±4.4	38.8±4.1	0.965	0.376	0.038
Minimum hip flexion	-2.5±5.8	-1.6±6.5	-2.1±6.2	0.294	0.642	0.222
Peak hip abduction swing	-5.9±2.4	-7.2±2.2	-5.8±2.3	**0.005**	0.905	**0.008**
Peak hip exorotation	-5.7±7.4	-4.4±5.9	-7.1±6.3	0.119	0.103	**<0.001**
Peak hip endorotation	9.2±8.4	9.0±5.3	5.3±5.1	0.904	0.095	**0.002**
ROM knee flexion	61.0±5.1	63.0±4.7	60.0±3.6	0.057	0.237	**<0.001**
Peak knee flexion swing	59.9±2.8	62.4±2.9	59.6±2.7	**<0.001**	0.195	**<0.001**
Peak knee extension stance	-0.2±3.7	0.2±3.8	0.6±3.2	0.726	0.444	0.499
Knee flexion at IC[2]	4.0±2.5	5.9±2.2	5.8±3.0	**0.027**	0.033	0.844
Time to peak knee flexion	72.2±0.4	72.2±0.4	72.2±0.4	1.000	1.000	1.000
Peak ankle dorsal stance	12.2±4.2	7.8±2.5	6.7±2.2	0.026	**0.003**	0.038
Peak ankle dorsal swing	8.4±1.5	5.0±2.6	2.2±2.5	**0.010**	**<0.001**	**<0.001**
Peak plantar push-off	4.8±5.1	0.7±5.0	-2.3±4.3	**0.007**	**<0.001**	**<0.001**

Notes: [1]ROM – range of motion; [2]IC – initial contact;
Underlined results exceed MCID ($5°$).

4 Discussion

The objectives of this study were, firstly, to analyse the differences between biomechanical models definitions used in gait analysis; secondly, to harmonise models and, thirdly, assess whether the harmonised joint angles kinematics result in improved outcomes comparability.

The biomechanical analysis started by collecting motion capture data, consisting in 3D markers trajectories of participants performing walking task. Three biomechanical models (CGM, CAST and LAMB) were implemented to obtain joint angles kinematics. The models' definitions were analysed both during the calibration and task trials, by comparing each segment AFs between two biomechanical models. The differences between two AFs were quantified as rotational and translational offsets. The harmonisation processes consisted in CT between respective AFs and OpenSim IK. Joint angles kinematic curves and parameters were obtained for native and harmonised models.

Interpretation of anatomical frames differences

Biomechanical models definitions differences consist in a rotational offset between two axes, and a translational offset between AFs' origins. Pelvis definitions are the most consistent between all models, while all the other segments' AFs differ considerably. Both offsets, rotational and translational, show higher differences between models than between subjects, suggesting a systematic difference between two models. More importantly, the offsets are not constant across the gait cycle. Therefore, the difference between biomechanical models' is a nonlinear function of the gait cycle. This variability is also represented by the inconsistency between AFs' origins. Thigh and shank share both the same origins definition: KJC and AJC, calculated as midpoints between epicondyles and malleoli, respectively. AFs from the calibration trial show the origins overlapping. However, during the task trials, the two points are shifted. Both, KJC and AJC, are calculated during the calibration trial and their position is recorded in the respective thigh and shank TFs. The position of the two points is then reconstructed, through anatomical calibration, in the task trial in each frame, based on the assumption that this position does not shift with respect to the TF. However, in each model, different markers are used to define the TFs, each with different amount of STA, which can reach few centimeters [10, 40, 41, 42, 43, 44]. Therefore, as STA varies for each marker, the markers positions are influenced with respect to the underlying bone, but also with respect to other markers used to define the TF in consideration [9, 10, 45]. *Gao et al.* [46] showed an inter-markers movements up to 19.1mm and 9.3mm on thigh and shank segments, respectively, during level walking. The inter-markers movements apply for CGM and LAMB TFs. CAST thigh and shank TFs are defined by using markers attached to the rigid plate, which implies that all markers on the plate are influenced by the STA with respect to the bone, but the distance between markers on the plate is constant (unless instrumental error). STA is also lower for markers positioned on a plate [10, 44] and the instrumental error is lower than the error introduced by STA [10]. Moreover, STA is greater at the thigh [41, 42, 44, 45], in particular in the joint line proximity, and it is proportional to the joint's motion [9, 41, 42, 45, 46], which explains the

higher inconsistency in the thigh AFs. Moreover, STA was found to be in a nonlinear relationship with the knee flexion/extension angle [41, 47] and markers displacement is also correlated to hip flexion angle [48].

A maximum translational offset of 41mm was found in this study relative to the thigh AFs (i.e. translation between KJCs), which is consistent with a thigh marker position displacement associated with STA found in [10, 34] – 40mm, and at the knee joint line in [45] – 40mm.

The high translation between foot AFs is due to different origins definitions: AJC for CGM and LAMB and CA marker for CAST. However, despite the same definition, a translation is observed also between CGM and LAMB foot AFs origins as different markers are involved in the TFs definitions. This does not apply for the pelvis AFs, as each biomechanical model considers the same pelvis markers.

Harmonisation analysis

Coordinate Transformation

The advantage of a merged markerset allows to calculate joint kinematics with different biomechanical models for the exact same gait cycle. Therefore, a native outcome was used as reference for the harmonised results comparison. Moreover, the subject involved in harmonisation was not included in the transformation matrix calculation to avoid biased results.

The CT was performed by calculating the transformation matrix for each frame of the task trial, as mean of all frames and by considering the calibration trial. The frame-by-frame harmonisation provides joint kinematics comparable with the native model's outcomes. This harmonisation also results in more comparable outcomes than mean or static harmonisations. As illustrated in the previous section, a systematic difference between models' definition was found and this difference varies nonlinearly as function of the gait cycle. This difference is attributed to STA, which, during walking task, can reduce the ROM and influence the hip joint angle up 7.3° on the sagittal plane [44] and knee joint angle up to 7.4° and 7.5° on frontal and transverse planes, respectively [42]. In both studies the kinematics curves were compared to results obtained with fluoroscopy and both concluded that STA influences joint kinematics mostly on out-of-sagittal planes. Therefore, a dynamic transformation performed for each frame accounts for this systematic difference.

If markers were rigidly attached to the body (i.e. no STA), the static harmonisation would provide the output equal to the native model's. Static harmonisation improves the outputs' consistency, but, it is not equal. Therefore, the transformations are different for each segment AFs, defined by different markers and TFs. If the difference between models would be only due to instrumental error [4], the mean harmonisation would provide an equal output. Mean harmonisation improves the outputs' consistency, but not completely as the difference between models was found to vary across the gait cycle with a nonlinear pattern.

The statistically significant differences in the two harmonisations, static and mean, are found in terminal stance and during swing phase, both associated with increased STA due to higher

knee flexion angle [9, 41, 42]. The frame-by-frame harmonisation accounts for the variability in biomechanical models' definitions due to the different amount of STA between different markers and the underlying bone. However, the output still presents some inconsistencies, which are not statistically or clinically different. This is attributed to different subject providing different transformations due to subject-dependent STA [9, 40, 41, 42, 44].

OpenSim Inverse Kinematics

IK offers a systematic approach to describe any biomechanical model, it matches the subject's anatomy and allows for more flexibility in markers placements and STA reduction [2, 9, 17]. By introducing constraints at the joint between segments, the results are more reliable [17, 21]. According to *Roelker et al.* [24] Gait2392 model is enough for healthy subjects assessment. *Kainz et al.* [21, 49] argue it is not enough for clinical gait analysis due to the reduced number of DoFs on frontal and transverse planes. However, *Leardini et al.* [9] emphasises that the errors due to the STA on frontal and transverse planes have comparable or even higher magnitude than the joint motion, therefore, those angles cannot be accurately measured with marker-based motion analysis. These errors are confirmed by the fluoroscopy study of the knee [42].

The IK model used in this study is Gait2352 with 3-1-1 DoFs at hip, knee and ankle respectively. The difference between Gait2354 and Gait2392 is in the number of muscles, therefore, Gait2352 is enough to assess healthy subjects kinematics. The same underlying model was used for the IK joint angles calculation and according to *Kainz et al.* [21] the variability is lower when the same model is used. The comparability between the three biomechanical models' markersets is high on all planes with consistent waveform patterns. These results are in contrast with *Mantovani et al.* [50], where different markersets produced non comparable results, especially on transverse plane, with the CGM markerset being the most variable. However, in the aforementioned study, CGM was compared to different markersets than those included in this study. Moreover, *Mantovani et al.* calculated the joint centers according to each biomechanical model's definitions and considered the joint centers as virtual markers in the OpenSim model. The differences in joint kinematics were attributed to anatomical markers used to define the joint centers. In this study, no additional markers or joint centers were calculated and only TMs were used for the IK, thus, eliminating the variability due to different joint centers definitions. Therefore, by limiting the IK to tracking only TMs, joint kinematics results are more consistent when different markersets are implemented. *Kainz et al.* [21], concluded that scaling is more accurate when based on joint centers, but no effects on joint kinematics were investigated. Finally, *Mantovani et al.* considered a 3-3-2 DoFs model on hip, knee and ankle respectively. In this study, the OpenSim model has only 3-1-1 DoFs, therefore, differences on out-of-sagittal planes knee and ankle kinematics due to different markersets could not be compared.

Only the ankle joint angles differences were higher than MCID when CGM markerset was included in the comparison. CGM markerset has only two markers on the foot, which influences the tracking accuracy, as at least three markers should be used to correctly calculate the segment's pose.

Limitations and recommendations for a follow-up study

Although the operator involved in the experiments (i.e. the author) was trained during the experiments by a physiotherapist with 15 years experience, the kinematic outcomes from the native models presents higher variability than reported in literature by [27, 30]. The kinematic outcomes of this study are more consistent with the results from *Benedetti et al.* [28], where the variability between operators is included in the analysis. The inter-operators inconsistency in markers placement (of 10mm) reaches a RMSE in joint kinematics up to 25° [20] and the problematic plate markers alignment results in vertical shift in the hip angle on the sagittal plane [33] and inconsistencies in the angles on the frontal and transverse planes [21]. Therefore, the operator's inconsistency, mainly due to inexperience [26], in markers placement influenced the results from the native models [51, 52, 53, 54]. It is recommended to train the operator prior the experiments [52]. However, the variability due to different operators should be also included in further studies. Therefore, from this perspective, it is advantageous the operator was not an expert and introduced more variability in the markers placement.

This study included only three biomechanical models, while for a better overview more models should be analysed and transformation matrices calculated. Moreover, as CGM presents different variants [55], the effect of different model's implementation on the harmonisation should be investigated, with the focus on variants that produce more accurate results (e.g. knee alignment devices, HJC Harrington equations). The implemented here CGM presents a modification with respect to the current PiG implemented in Nexus[6], which consists in estimating the KJC and AJC as midpoints between epicondyles and malleoli respectively. The current PiG model uses a chord function which allows for dynamic, frame-by-frame, estimation of the joint centers based on a previously calculated joint center, a wand/plate marker and a lateral marker. The accuracy of this dynamic estimation with respect to the STA and harmonisation process should be included in further analysis.

This study did not address the models' reliability and accuracy and the implemented models present some simplifications with respect to current state of the models implementations. For example, HJC estimation is more accurate with Harrington equations [56], implemented in the open source updated CGM (pyCGM2) [36]. Moreover, optimisation algorithms have been also proposed to increase repeatability of biomechanical models and to minimise STA, with successful outcomes [12, 20]. Future studies should take into account the current models' implementation and optimisation techniques.

The harmonisation methods presented in this study were analysed by considering healthy population. As clinical gait analysis involves a wide variety of impaired populations, the transformations from one model to another should be investigated. It should be determined whether the same universal transformation matrices, as obtained in this study for healthy subjects, can be applied for impaired subjects and whether the transformation matrix and the STA vary according to different pathologies. Although this study did not consider kinetic outcome as their repeatability was found to be consistent when different biomechanical models are implemented [27], future

[6] Plug-in Gait Reference Guide

studies should also assess the comparability of kinetic outcomes from harmonised kinematic results.

The joint angles kinematics are less comparable on out-of-sagittal planes, however, only four kinematic parameters were used on those planes. Therefore, more kinematic parameters on frontal and transverse planes should be included in order to describe the curves in details and capture the waveform potential opposite patterns. Moreover, the OpenSim IK model used in this study implements only one DoF for knee and ankle joints. It is argued that the reduced number of DoFs is not sufficient for clinical assessment, however, the error on frontal and transverse planes can be higher than the angles' ROM. Therefore, consensus is needed in the biomechanical community regarding whether frontal and transverse planes joint angles should be included in the analysis, despite the accuracy that can be currently achieved.

The frame-by-frame harmonisation depends on the gait cycle detection. It is important that the event detection procedure provides comparable results, as any shift can interfere with the harmonisation process effectiveness. This factor is of particular relevance when harmonisation matrices are calculated in one laboratory and applied in another one, which implements a different gait event detection method.

In order to quantify the effect of STA on AFs, but also on TFs, 3D fluoroscopy should be used together with stereophotogrammetric cameras, as in [40, 41, 44]. Several biomechanical models and markersets should be implemented simultaneously and analysed during the same gait cycle. With this technique, STA behaviour could be quantified for each biomechanical model definitions for AFs, TFs and single markers. Bone intracortical pins are not suggested as this technique is highly invasive and bone pins limit and alter STA behavior [40, 46].

Finally, quantitative comparison is needed to determine which approach, CT or IK, is most suitable for data harmonisation. According to *Kainz et al.* [57], when cerebral palsy patients are evaluated, CGM and IK provide comparable outputs with similar kinematic waveforms, even when more DoFs are included in the IK model. However, both approaches vary conceptually and there is no agreement in the biomechanical community on which is more suitable for clinical gait analysis. IK approach is considered more human-like as it implements an anatomically based model. However, there is who argue certain joint assumptions (e.g. knee as hinge joint) depend on the research's purpose, and in general, are not accurate enough for clinical analysis. Biomechanical models are dependent on markers accurate and repeatable placement and are highly influenced by the STA. Therefore, more agreement is needed for the sake of data comparability, although all harmonisation methods presented here could improve data sharing and comparability by allowing easily to switch between models.

5 Conclusions

The goals of this study were to assess the differences between biomechanical models' definitions and to harmonise these models through coordinate transformation (CT) and inverse kinematics (IK). Three widely adopted biomechanical models (CGM ,CAST, LAMB) were implemented and analysed. Differences, as rotational and translational offsets, up to 23.3° and 41mm were found between AFs. Moreover, a systematic difference was found between models, as nonlinear function of the gait cycle.

CT harmonisation was performed for three transformation matrices calculations: frame-by-frame (dynamic from task trial), mean across task trial gait cycle and static (from calibration trial). Each harmonisation improved the joint angles kinematics, with frame-by-frame harmonisation providing the best results. This is in accordance with the systematic difference found between models, as frame-by-frame harmonisation takes into account this variability between biomechanical models' definitions across the gait cycle. IK harmonisation provides comparable results, with clinically significant difference only for the ankle flexion-extension angle, identified as vertical shift, when the model's definitions include only two markers to track the foot's motion.

The main reason for the systematic difference is suggested to be STA, which varies for different markers and subjects. However, further investigation is needed to quantify STA with respect to each model's AFs and TFs definitions by using stereophotogrammetry and fluoroscopy simultaneously.

A clear insight in biomechanical models' differences and the consequent inconsistencies in joint angles kinematics were illustrated. This study provides a promising methodology for biomechanical models harmonisation, which provides comparable outcomes. The harmonisation allows to easily switch between biomechanical models: only several measurements with two models implemented simultaneously are needed and the calculation of the universal transformation matrices. This method is particularly meaningful for clinical practice as it can improve data comparability and sharing and, consequently, allow further innovation in gait analysis methodology. As patients data should be compared with normative data obtained from the same biomechanical model, with the harmonisation, there is no need for multiple normative datasets. The harmonisation presented in this study could be implemented in data sharing repositories, such as GaitaBase [58], and account for biomechanical models differences and, therefore, enhance the dataset reliability.

As no biomechanical model can be considered as ground truth, the harmonisation techniques allow data comparability between different gait laboratories without gaining consensus in the biomechanical community regarding which model should be considered superior. Nevertheless, further investigation of soft tissue artefact effects on biomechanical models' definitions and consequent joint kinematics will yield a model closely approximating the ground truth.

References

[1] T. A. Wren, G. E. Gorton III, S. Ounpuu, and C. A. Tucker, "Efficacy of clinical gait analysis: A systematic review," *Gait & posture*, vol. 34, no. 2, pp. 149–153, 2011.

[2] R. Baker, *Measuring walking: a handbook of clinical gait analysis*. Mac Keith Press, 2013.

[3] A. Cappozzo, U. Della Croce, A. Leardini, and L. Chiari, "Human movement analysis using stereophotogrammetry: Part 1: theoretical background," *Gait & posture*, vol. 21, no. 2, pp. 186–196, 2005.

[4] L. Chiari, U. Della Croce, A. Leardini, and A. Cappozzo, "Human movement analysis using stereophotogrammetry: Part 2: Instrumental errors," *Gait & posture*, vol. 21, no. 2, pp. 197–211, 2005.

[5] J. Dicharry, "Kinematics and kinetics of gait: from lab to clinic," *Clinics in sports medicine*, vol. 29, no. 3, pp. 347–364, 2010.

[6] G. Wu and P. R. Cavanagh, "Isb recommendations for standardization in the reporting of kinematic data," *Journal of biomechanics*, vol. 28, no. 10, pp. 1257–1261, 1995.

[7] G. Wu, S. Siegler, P. Allard, C. Kirtley, A. Leardini, D. Rosenbaum, M. Whittle, D. D D'Lima, L. Cristofolini, H. Witte, *et al.*, "Isb recommendation on definitions of joint coordinate system of various joints for the reporting of human joint motion—part i: ankle, hip, and spine," *Journal of biomechanics*, vol. 35, no. 4, pp. 543–548, 2002.

[8] A. Cappozzo, "Gait analysis methodology," *Human movement science*, vol. 3, no. 1-2, pp. 27–50, 1984.

[9] A. Leardini, L. Chiari, U. Della Croce, and A. Cappozzo, "Human movement analysis using stereophotogrammetry: Part 3. soft tissue artifact assessment and compensation," *Gait & posture*, vol. 21, no. 2, pp. 212–225, 2005.

[10] A. Leardini, C. Belvedere, F. Nardini, N. Sancisi, M. Conconi, and V. Parenti-Castelli, "Kinematic models of lower limb joints for musculo-skeletal modelling and optimization in gait analysis," *Journal of biomechanics*, vol. 62, pp. 77–86, 2017.

[11] A. Cappozzo, F. Catani, U. Della Croce, and A. Leardini, "Position and orientation in space of bones during movement: anatomical frame definition and determination," *Clinical biomechanics*, vol. 10, no. 4, pp. 171–178, 1995.

[12] I. Charlton, P. Tate, P. Smyth, and L. Roren, "Repeatability of an optimised lower body model," *Gait & Posture*, vol. 20, no. 2, pp. 213–221, 2004.

[13] M. Kadaba, H. Ramakrishnan, and M. Wootten, "Measurement of lower extremity kinematics during level walking," *Journal of orthopaedic research*, vol. 8, no. 3, pp. 383–392, 1990.

[14] R. B. Davis, S. Ounpuu, D. Tyburski, and J. R. Gage, “A gait analysis data collection and reduction technique,” 1991.

[15] M. G. Benedetti, F. Catani, A. Leardini, E. Pignotti, and S. Giannini, “Data management in gait analysis for clinical applications,” *Clinical biomechanics*, vol. 13, no. 3, pp. 204–215, 1998.

[16] M. Rabuffetti, A. Marzegan, A. Crippa, I. Carpinella, T. Lencioni, A. Castagna, and M. Ferrarin, “The lamb gait analysis protocol: Definition and experimental assessment of operator-related variability,” *Proceedings of the Institution of Mechanical Engineers, Part H: Journal of engineering in medicine*, vol. 233, no. 3, pp. 342–353, 2019.

[17] T.-W. Lu and J. O’connor, “Bone position estimation from skin marker co-ordinates using global optimisation with joint constraints,” *Journal of biomechanics*, vol. 32, no. 2, pp. 129–134, 1999.

[18] S. L. Delp, F. C. Anderson, A. S. Arnold, P. Loan, A. Habib, C. T. John, E. Guendelman, and D. G. Thelen, “Opensim: open-source software to create and analyze dynamic simulations of movement,” *IEEE transactions on biomedical engineering*, vol. 54, no. 11, pp. 1940–1950, 2007.

[19] S. Duprey, L. Cheze, and R. Dumas, “Influence of joint constraints on lower limb kinematics estimation from skin markers using global optimization,” *Journal of biomechanics*, vol. 43, no. 14, pp. 2858–2862, 2010.

[20] B. E. Groen, M. Geurts, B. Nienhuis, and J. Duysens, “Sensitivity of the olga and vcm models to erroneous marker placement: Effects on 3d-gait kinematics,” *Gait & posture*, vol. 35, no. 3, pp. 517–521, 2012.

[21] H. Kainz, D. Graham, J. Edwards, H. P. Walsh, S. Maine, R. N. Boyd, D. G. Lloyd, L. Modenese, and C. P. Carty, “Reliability of four models for clinical gait analysis,” *Gait & posture*, vol. 54, pp. 325–331, 2017.

[22] A. Seth, M. Sherman, J. A. Reinbolt, and S. L. Delp, “Opensim: a musculoskeletal modeling and simulation framework for in silico investigations and exchange,” *Procedia Iutam*, vol. 2, pp. 212–232, 2011.

[23] A. J. Van den Bogert, T. Geijtenbeek, O. Even-Zohar, F. Steenbrink, and E. C. Hardin, “A real-time system for biomechanical analysis of human movement and muscle function,” *Medical & biological engineering & computing*, vol. 51, no. 10, pp. 1069–1077, 2013.

[24] S. A. Roelker, E. J. Caruthers, R. K. Baker, N. C. Pelz, A. M. Chaudhari, and R. A. Siston, “Interpreting musculoskeletal models and dynamic simulations: causes and effects of differences between models,” *Annals of biomedical engineering*, vol. 45, no. 11, pp. 2635–2647, 2017.

[25] S. L. Delp, J. P. Loan, M. G. Hoy, F. E. Zajac, E. L. Topp, and J. M. Rosen, "An interactive graphics-based model of the lower extremity to study orthopaedic surgical procedures," *IEEE Transactions on Biomedical engineering*, vol. 37, no. 8, pp. 757–767, 1990.

[26] J. L. McGinley, R. Baker, R. Wolfe, and M. E. Morris, "The reliability of three-dimensional kinematic gait measurements: a systematic review," *Gait & posture*, vol. 29, no. 3, pp. 360–369, 2009.

[27] A. Ferrari, M. G. Benedetti, E. Pavan, C. Frigo, D. Bettinelli, M. Rabuffetti, P. Crenna, and A. Leardini, "Quantitative comparison of five current protocols in gait analysis," *Gait & posture*, vol. 28, no. 2, pp. 207–216, 2008.

[28] M. Benedetti, A. Merlo, and A. Leardini, "Inter-laboratory consistency of gait analysis measurements," *Gait & posture*, vol. 38, no. 4, pp. 934–939, 2013.

[29] K. Kaufman, E. Miller, T. Kingsbury, E. R. Esposito, E. Wolf, J. Wilken, and M. Wyatt, "Reliability of 3d gait data across multiple laboratories," *Gait & posture*, vol. 49, pp. 375–381, 2016.

[30] E. Flux, M. van der Krogt, P. Cappa, M. Petrarca, K. Desloovere, and J. Harlaar, "The human body model versus conventional gait models for kinematic gait analysis in children with cerebral palsy," *Human Movement Science*, vol. 70, p. 102585, 2020.

[31] V. Camomilla, R. Dumas, and A. Cappozzo, "Human movement analysis: The soft tissue artefact issue," 2017.

[32] K. J. Noonan, S. Halliday, R. Browne, S. O'Brien, K. Kayes, and J. Feinberg, "Interobserver variability of gait analysis in patients with cerebral palsy," *Journal of Pediatric Orthopaedics*, vol. 23, no. 3, pp. 279–287, 2003.

[33] M. Kadaba, H. Ramakrishnan, M. Wootten, J. Gainey, G. Gorton, and G. Cochran, "Repeatability of kinematic, kinetic, and electromyographic data in normal adult gait," *Journal of orthopaedic research*, vol. 7, no. 6, pp. 849–860, 1989.

[34] A. Cappozzo, F. Catani, A. Leardini, M. Benedetti, and U. Della Croce, "Position and orientation in space of bones during movement: experimental artefacts," *Clinical biomechanics*, vol. 11, no. 2, pp. 90–100, 1996.

[35] A. Leardini, A. Cappozzo, F. Catani, S. Toksvig-Larsen, A. Petitto, V. Sforza, G. Cassanelli, and S. Giannini, "Validation of a functional method for the estimation of hip joint centre location," *Journal of biomechanics*, vol. 32, no. 1, pp. 99–103, 1999.

[36] F. Leboeuf, R. Baker, A. Barré, J. Reay, R. Jones, and M. Sangeux, "The conventional gait model, an open-source implementation that reproduces the past but prepares for the future," *Gait & posture*, vol. 69, pp. 235–241, 2019.

[37] A. Falisse, S. Van Rossom, J. Gijsbers, F. Steenbrink, B. J. van Basten, I. Jonkers, A. J. van den Bogert, and F. De Groote, "Opensim versus human body model: a comparison study for the lower limbs during gait," *Journal of applied biomechanics*, vol. 34, no. 6, pp. 496–502, 2018.

[38] J. de Winter and D. Dodou, "Pitfalls of statistical methods in traffic psychology," 2020.

[39] J. M. Wilken, K. M. Rodriguez, M. Brawner, and B. J. Darter, "Reliability and minimal detectible change values for gait kinematics and kinetics in healthy adults," *Gait & posture*, vol. 35, no. 2, pp. 301–307, 2012.

[40] R. Stagni, S. Fantozzi, A. Cappello, and A. Leardini, "Quantification of soft tissue artefact in motion analysis by combining 3d fluoroscopy and stereophotogrammetry: a study on two subjects," *Clinical Biomechanics*, vol. 20, no. 3, pp. 320–329, 2005.

[41] T.-Y. Tsai, T.-W. Lu, M.-Y. Kuo, and H.-C. Hsu, "Quantification of three-dimensional movement of skin markers relative to the underlying bones during functional activities," *Biomedical Engineering: Applications, Basis and Communications*, vol. 21, no. 03, pp. 223–232, 2009.

[42] M. Akbarshahi, A. G. Schache, J. W. Fernandez, R. Baker, S. Banks, and M. G. Pandy, "Non-invasive assessment of soft-tissue artifact and its effect on knee joint kinematics during functional activity," *Journal of biomechanics*, vol. 43, no. 7, pp. 1292–1301, 2010.

[43] A. Barré, B. M. Jolles, N. Theumann, and K. Aminian, "Soft tissue artifact distribution on lower limbs during treadmill gait: influence of skin markers' location on cluster design," *Journal of biomechanics*, vol. 48, no. 10, pp. 1965–1971, 2015.

[44] N. M. Fiorentino, P. R. Atkins, M. J. Kutschke, J. M. Goebel, K. B. Foreman, and A. E. Anderson, "Soft tissue artifact causes significant errors in the calculation of joint angles and range of motion at the hip," *Gait & posture*, vol. 55, pp. 184–190, 2017.

[45] A. Peters, B. Galna, M. Sangeux, M. Morris, and R. Baker, "Quantification of soft tissue artifact in lower limb human motion analysis: a systematic review," *Gait & posture*, vol. 31, no. 1, pp. 1–8, 2010.

[46] B. Gao and N. N. Zheng, "Investigation of soft tissue movement during level walking: translations and rotations of skin markers," *Journal of Biomechanics*, vol. 41, no. 15, pp. 3189–3195, 2008.

[47] E. H. Garling, B. L. Kaptein, B. Mertens, W. Barendregt, H. Veeger, R. G. Nelissen, and E. R. Valstar, "Soft-tissue artefact assessment during step-up using fluoroscopy and skin-mounted markers," *Journal of biomechanics*, vol. 40, pp. S18–S24, 2007.

[48] R. Hara, M. Sangeux, R. Baker, and J. McGinley, "Quantification of pelvic soft tissue artifact in multiple static positions," *Gait & Posture*, vol. 39, no. 2, pp. 712–717, 2014.

[49] H. Kainz, H. X. Hoang, C. Stockton, R. R. Boyd, D. G. Lloyd, and C. P. Carty, "Accuracy and reliability of marker-based approaches to scale the pelvis, thigh, and shank segments in musculoskeletal models," *Journal of applied biomechanics*, vol. 33, no. 5, pp. 354–360, 2017.

[50] G. Mantovani and M. Lamontagne, "How different marker sets affect joint angles in inverse kinematics framework," *Journal of biomechanical engineering*, vol. 139, no. 4, 2017.

[51] U. Della Croce, A. Leardini, L. Chiari, and A. Cappozzo, "Human movement analysis using stereophotogrammetry: Part 4: assessment of anatomical landmark misplacement and its effects on joint kinematics," *Gait & posture*, vol. 21, no. 2, pp. 226–237, 2005.

[52] G. E. Gorton III, D. A. Hebert, and M. E. Gannotti, "Assessment of the kinematic variability among 12 motion analysis laboratories," *Gait & posture*, vol. 29, no. 3, pp. 398–402, 2009.

[53] O. Pinzone, M. H. Schwartz, P. Thomason, and R. Baker, "The comparison of normative reference data from different gait analysis services," *Gait & posture*, vol. 40, no. 2, pp. 286–290, 2014.

[54] C. McFadden, K. Daniels, and S. Strike, "The sensitivity of joint kinematics and kinetics to marker placement during a change of direction task," *Journal of Biomechanics*, vol. 101, p. 109635, 2020.

[55] R. Baker, F. Leboeuf, J. Reay, M. Sangeux, *et al.*, "The conventional gait model-success and limitations," *Handbook of human motion. Cham: Springer International Publishing*, pp. 489–508, 2018.

[56] N. M. Fiorentino, M. J. Kutschke, P. R. Atkins, K. B. Foreman, A. L. Kapron, and A. E. Anderson, "Accuracy of functional and predictive methods to calculate the hip joint center in young non-pathologic asymptomatic adults with dual fluoroscopy as a reference standard," *Annals of biomedical engineering*, vol. 44, no. 7, pp. 2168–2180, 2016.

[57] H. Kainz, L. Modenese, D. Lloyd, S. Maine, H. Walsh, and C. Carty, "Joint kinematic calculation based on clinical direct kinematic versus inverse kinematic gait models," *Journal of biomechanics*, vol. 49, no. 9, pp. 1658–1669, 2016.

[58] O. Tirosh, R. Baker, and J. McGinley, "Gaitabase: Web-based repository system for gait analysis," *Computers in Biology and Medicine*, vol. 40, no. 2, pp. 201–207, 2010.

[59] E. S. Grood and W. J. Suntay, "A joint coordinate system for the clinical description of three-dimensional motions: application to the knee," *J Biomech Eng*, 1983.

Cover page: Eadweard Muybridge – Figure Hopping (1887)

A Theoretical Background: Joint Angles Calculation

In order to fully understand the CT harmonisation processes, it is important to describe how joint angles are obtained from markers 3D position.

In the DK approach, markers are placed on anatomical landmarks (ALs) or in arbitrary, but strategic locations (TMs), which allow complete visibility by the cameras and STA minimization. TMs can be also placed on ALs, however, the main difference is that some ALs might be removed during task trials, while TMs are all recorded during both calibration and task trials. Therefore, TMs are here referred also as *tracking* markers.

To describe a segment's position and orientation (i.e. pose) in space, at least three markers are needed to define the segment's local coordinate system. Therefore, TMs are used to define technical local frames (TF), while ALs are used to define anatomical local frames (AF) and are specific to each biomechanical model (Table B.2). Both coordinate systems represents transformation matrices from laboratory global frame (GF) to local frame TF and AF respectively: ${}_{GF}T_{TF}$ and ${}_{GF}T_{AF}$.

During calibration process, TFs and AFs are defined and relevant ALs location can be reconstructed in the TFs. This procedure allows for optimised markers placement as some ALs markers can be removed during the task trial. During task trials, the definition of TFs is repeated for each time frame and the respective AFs can be then reconstructed based on the calibration trial. The AFs of adjacent segments are used to compute the transformation matrix of the distal segment with respect to the proximal one. This transformation matrix can be decomposed in joint angles on anatomical planes [7, 59] and in a translation vector.

To summarise, for each body segment, joint angles calculations through marker-based DK approach are implemented as follows:

Calibration:

1. ALs and TMs recorded in GF
2. Global TMs position used to define TFs: ${}_{GF}T_{TF}$
3. ALs calculated in TF
4. According to Table B.2, ALs position in TFs are used to define AFs: ${}_{TF}T_{AF}$

Task trial:

1. TMs recorded in GF
2. TFs defined for each time frame
3. AFs are reconstructed in GF for each time frame, through TFs: ${}_{GF}T_{AF} = {}_{GF}T_{TF} * {}_{TF}T_{AF}$
4. For each time frame, transformation matrices ${}_{GF}T_{AF}$ of two adjacent segments are considered to compute the transformation: ${}_{prox}T_{dist} = {}_{GF}T_{AF(prox)^{-1}} * {}_{GF}T_{AF(dist)}$
5. ${}_{prox}T_{dist}$ represents the pose of the distal segment with respect the proximal one and can be decomposed in joint angles on anatomical planes

B Models Implementation

Table B.1: Merged markerset.

Marker[1]	Location	CGM	CAST	LAMB
$ASIS$	Anterior Superior Iliac Spine	TM, AL	TM, AL	TM, AL
$PSIS$	Posterior Superior Iliac Spine	TM, AL	TM, AL	TM, AL
$T1$	Plate (up)	-	TM	-
$T2$	Plate (anterior)	-	TM	TM
$T3$	Plate (posterior)	-	TM	-
THI	Plate (down)	TM	TM	-
GT	Great Trochanter	AL	AL	AL
LE	Lateral Epicondyle	TM, AL	AL	TM, AL
ME	Medial Epicondyle	AL	AL	AL
$S1$	Plate (up)	-	TM	-
$S2$	Plate (anterior)	-	TM	TM
$S3$	Plate (posterior)	-	TM	-
TIB	Plate (down)	TM	TM	-
HF	Head Fibulae	-	AL	TM
TT	Tibial Tuberosity	-	AL	-
LM	Lateral Malleolus	TM, AL	AL	TM, AL
MM	Medial Malleolus	AL	AL	AL
CA	Calcaneus	TM, AL	TM, AL	TM
FM	First Metatarsal Head	-	TM, AL	TM, AL
SM	Second Metatarsal Head	TM, AL	TM, AL	-
VM	Fifth Metatarsal Head	-	TM, AL	TM, AL
$C7$[2]	Cervical vertebrae C7	AL	AL	AL
$L5$[2]	Lumbar vertebrae L5	AL	AL	AL

Notes: TM – Tracking Marker: both technical and anatomical, used both in calibration and task trials; AL – Anatomical Landmark: used for AFs calculation;
[1] Lower limbs markers are placed on both sides of the subject: right and left;
[2] Used only in OpenSim scaling.

Table B.2: Models AFs definitions.

Model	Pelvis	Thigh	Shank	Foot	JCs
CGM[1]	$O = 0.5(RASIS + LASIS)$ $PSIS_{mid} = 0.5(RASIS + LPSIS)$ $y = RASIS - LASIS$ (r) $z = y \times (O - PSIS_{mid})$ (u) $x = z \times y$ (f)	$O = KJC$ $z = HJC - KJC$ (u) $k_f = LE - KJC$ (r) $x = z \times k_f$ (f) $y = x \times z$ (r)	$O = AJC$ $z = KJC - AJC$ (u) $k_f = LE - KJC$ (r) $x_{prox} = z \times k_f$ (f) $y_{prox} = x_{prox} \times z$ (r) $a_f = LM - AJC$ (r) $z_{dist} = z \times a_f$ (f) $y_{dist} = x_{dist} \times z$ (r)	$O = AJC$ $v = CA - SM$ $Z_G = [0, 0, 1]$ $z = (Z_G \times v) \times Z_g$ (b) $a_f = LM - AJC$ (r) $x = z \times a_f$ (u) $y = x \times z$ (r) +90° offset forward	HJC *Davis et al.* [14] $KJC = 0.5(LE + ME)$ $AJC = 0.5(LM + MM)$
CAST [11]	$O = 0.5(RASIS + LASIS)$ $PSIS_{mid} = 0.5(RPSIS + LPSIS)$ $qtp = (PSIS_{mid} - O) \times (RASIS - O)$ $y = RASIS - O$ (r) $x = qtp \times y$ (f) $z = y \times x$ (u)	$O = KJC$ $qfp = (FH - O) \times (LE - O)$ $z = FH - O$ (u) $y = qfp \times z$ (r) $x = z \times y$ (f)	$O = AJC$ $qfp = (HF - O) \times (LM - O)$ $qsp = qfp \times (TT - O)$ $z = qsp \times qfp$ (u) $y = qfp \times z$ (r) $x = z \times y$ (f)	$O = CA$ $qtp = (VM - O) \times (FM - O)$ $qsp = (SM - O) \times qtp$ $x = qtp \times qsp$ (f) $y = x \times qtp$ (r) $z = y \times x$ (u)	HJC *Leardini et al.* [35] $KJC = 0.5(LE + ME)$ $AJC = 0.5(LM + MM)$
LAMB [16]	$O = 0.5(RASIS + LASIS)$ $PSIS_{mid} = 0.5(RPSIS + LPSIS)$ $x = O - PSIS_{mid}$ (f) $z = (RASIS - LASIS) \times x$ (u) $y = x \times z$ (r)	$O = KJC$ $z = HJC - KJC$ (u) $x = z \times (LE - ME)$ (f) $y = x \times z$ (r)	$O = AJC$ $z = KJC - AJC$ (u) $x = z \times (LM - MM)$ (f) $y = x \times z$ (r)	$O = AJC$ $x = 0.5(FM + VM) - O$(f) $z = (VM - FM) \times x$ (u) $y = x \times z$ (r)	HJC *Davis et al.* [14] $KJC = 0.5(LE + ME)$ $AJC = 0.5(LM + MM)$

Notes: [1]Vicon Nexus (version 2.9), with two differences: the medio-lateral axis directed to the right and KJC and AJC are implemented here as midpoints between epicondyles and malleoli, respectively, not as a chord function, which is used in Vicon Nexus;
(r) – to the right, (u) – upward, (f) – forward;
qfp – quasi-frontal plane, qsp – quasi-sagittal plane, qtp – quasi-transverse plane;
All models implement Cardan angle convention with the following sequence: flexion/extension → abduction/adduction → internal/external rotation.

Table B.3: OpenSim scaling factors based on markers location.

Segment	**Marker pair**		
	Antero-posterior	Superior-inferior	Medial-lateral
Pelvis	RASIS-RPSIS/LASIS-LPSIS	RASIS-RGT/LASIS-LGT	RASIS-LASIS
Thigh	RLE-RME/LLE-LME	RASIS-RLE/LASIS-LLE	RLE-RME/LLE-LME
Shank	RLM-RMM/LLM-LMM	RLE-RME/LLE-LME	RLM-RMM/LLM-LMM
Foot	RCA-RFM/LCA-LFM	RCA-RLM/LCA-LLM	RFM-RVM/LFM-LVM
Torso	Unassigned	C7-L5	Unassigned

Table B.4: OpenSim scaling weights, adapted from [37].

Marker[1]	**Weight**
C7, L5	10
ASIS, PSIS	25
LE, ME, LM, MM	15
FM, SM, VM	4
CA, GT	10

Notes: [1]The marker weights were used on right and left sides.

C Results

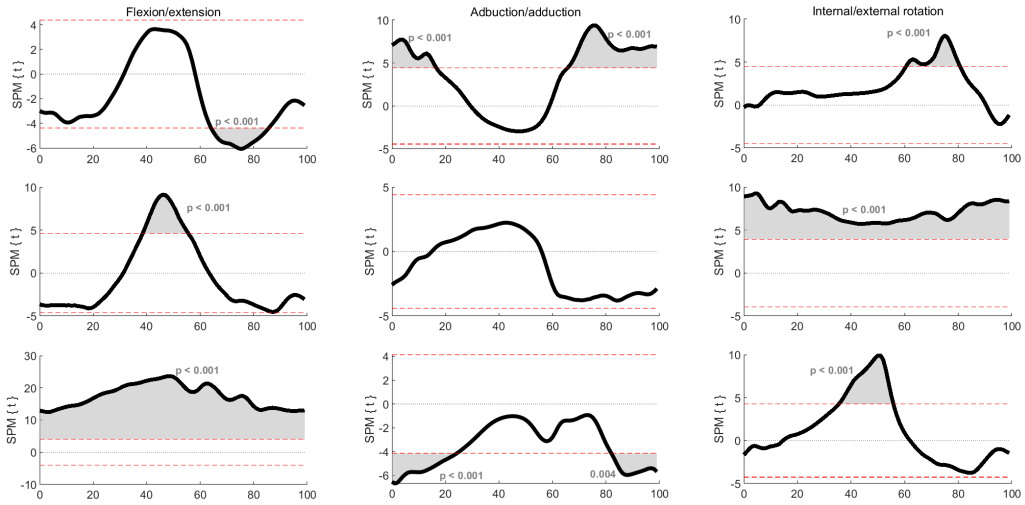

Figure C.1: Paired t-test results for LAMB-CGM comparison, obtained from SPM.

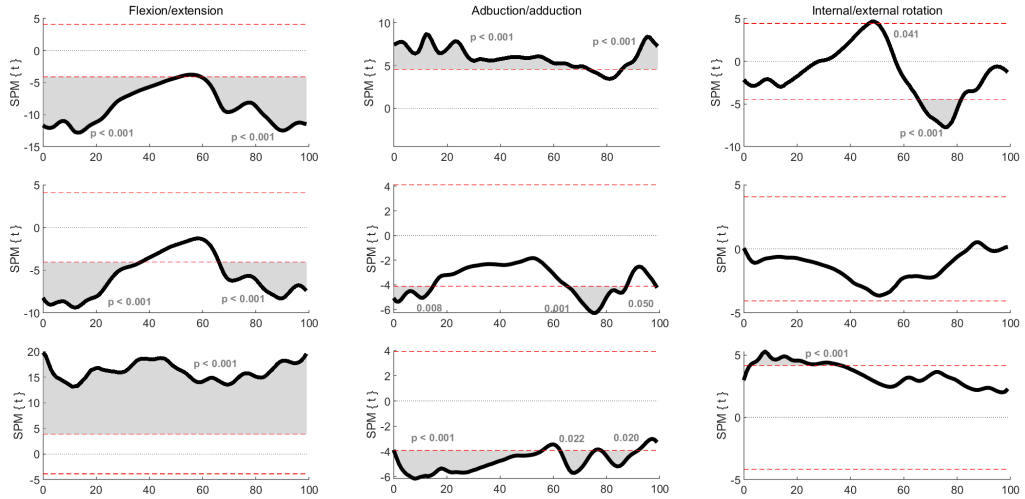

Figure C.2: Paired t-test results for CAST-LAMB comparison, obtained from SPM.

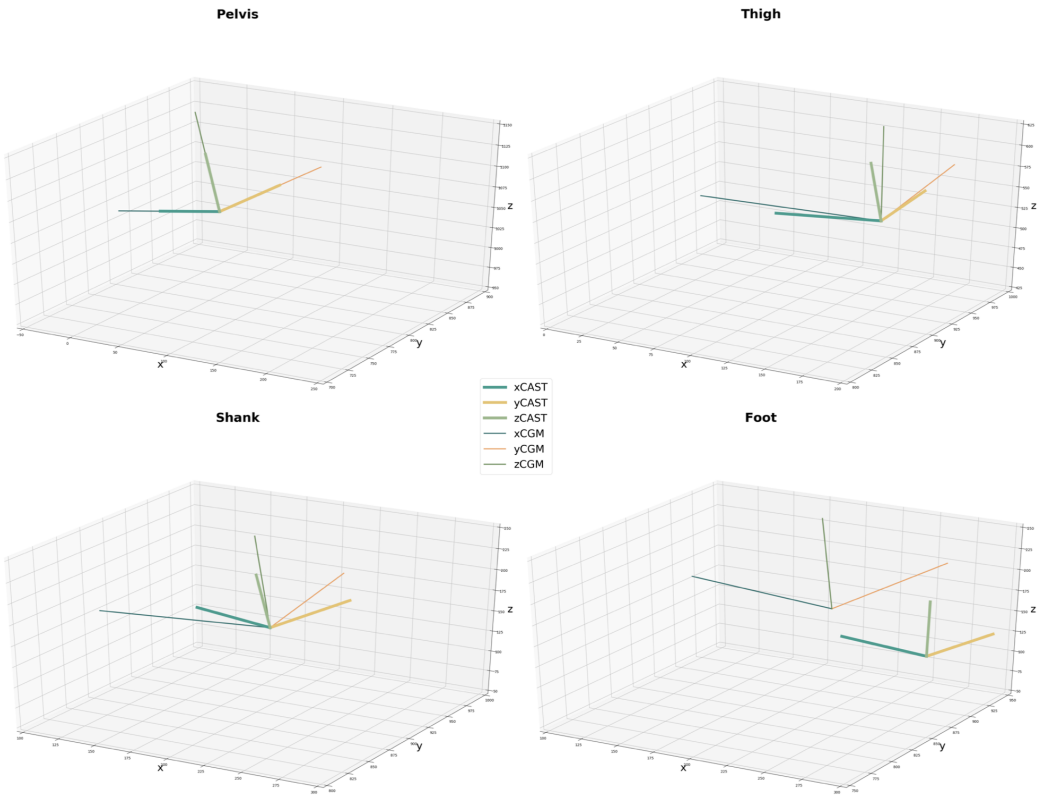

Figure C.3: Anatomical Frames (AFs) for each segment for CGM and CAST calculated during the calibration trial.

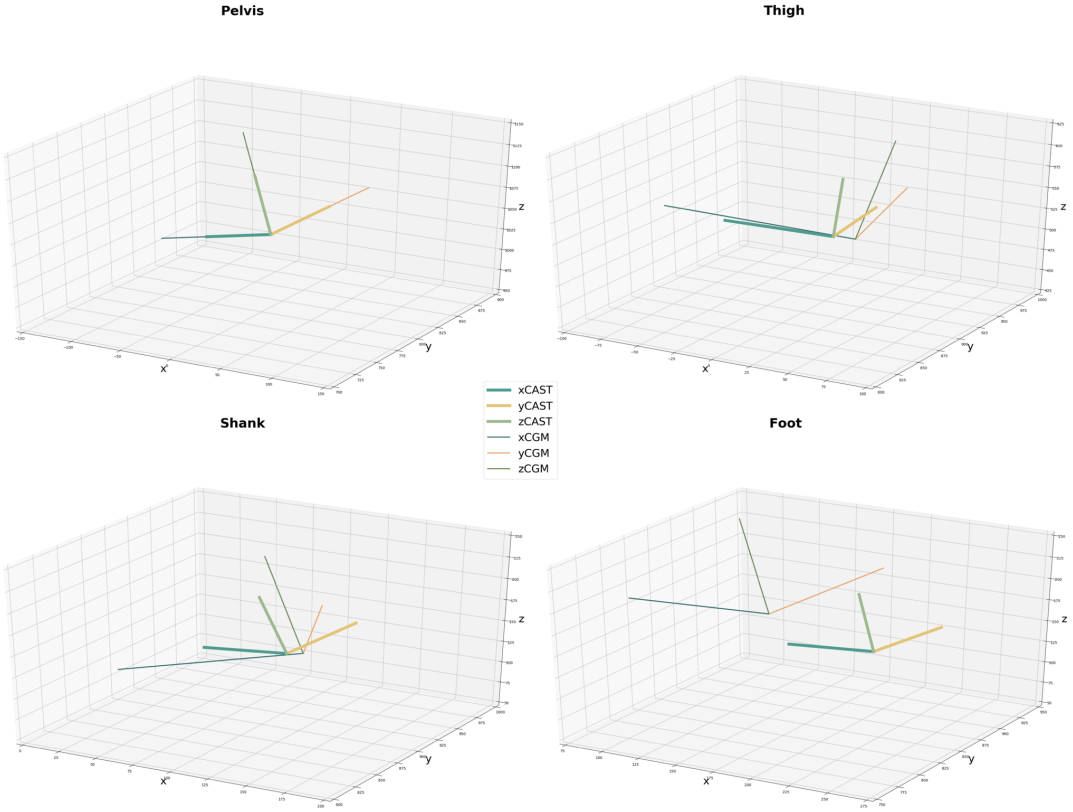

Figure C.4: Anatomical Frames (AFs) for each segment for CGM and CAST calculated as mean across all frames during the task trial.

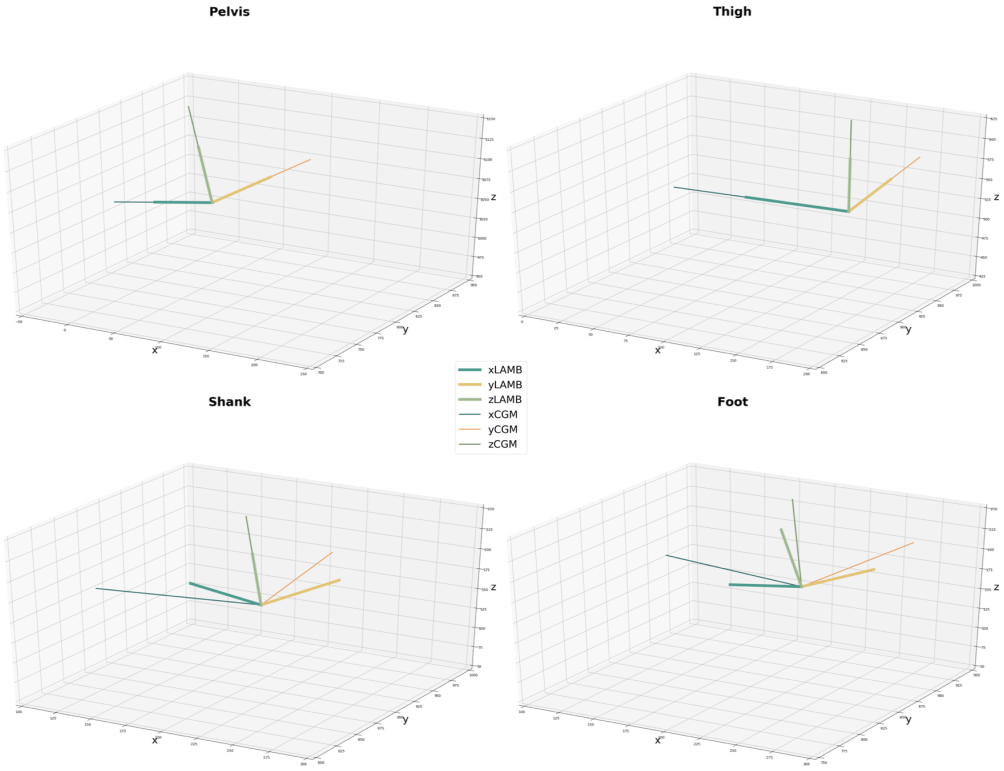

Figure C.5: Anatomical Frames (AFs) for each segment for CGM and LAMB calculated during the calibration trial.

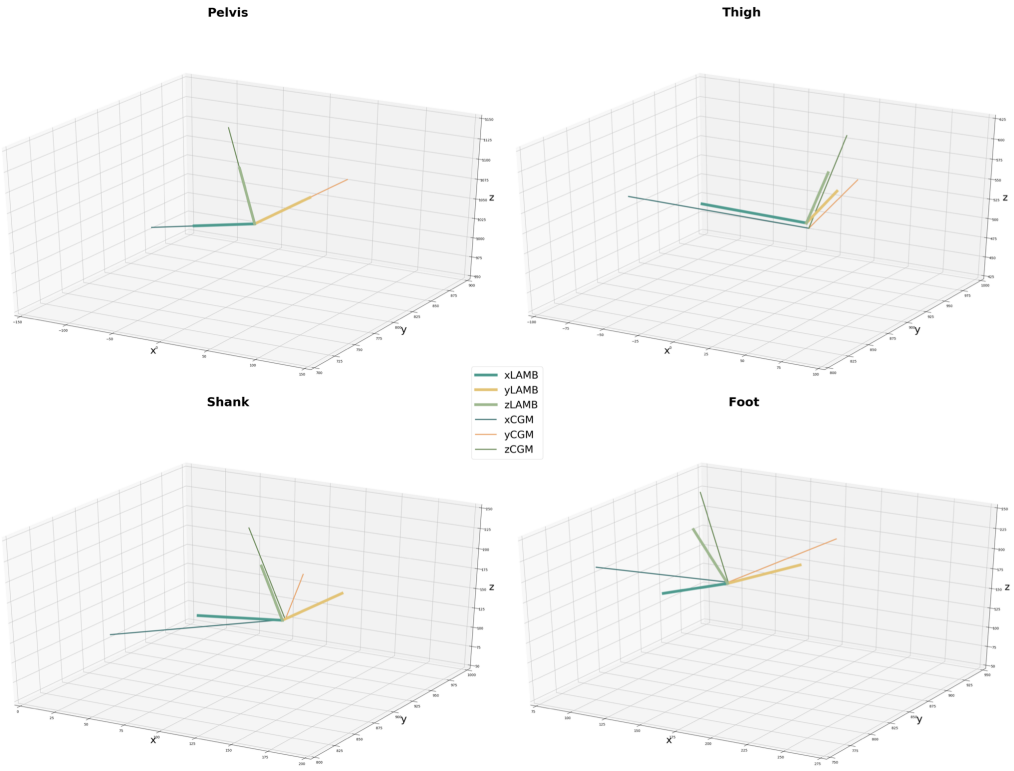

Figure C.6: AFs for each segment for CGM and LAMB calculated during the task trial.

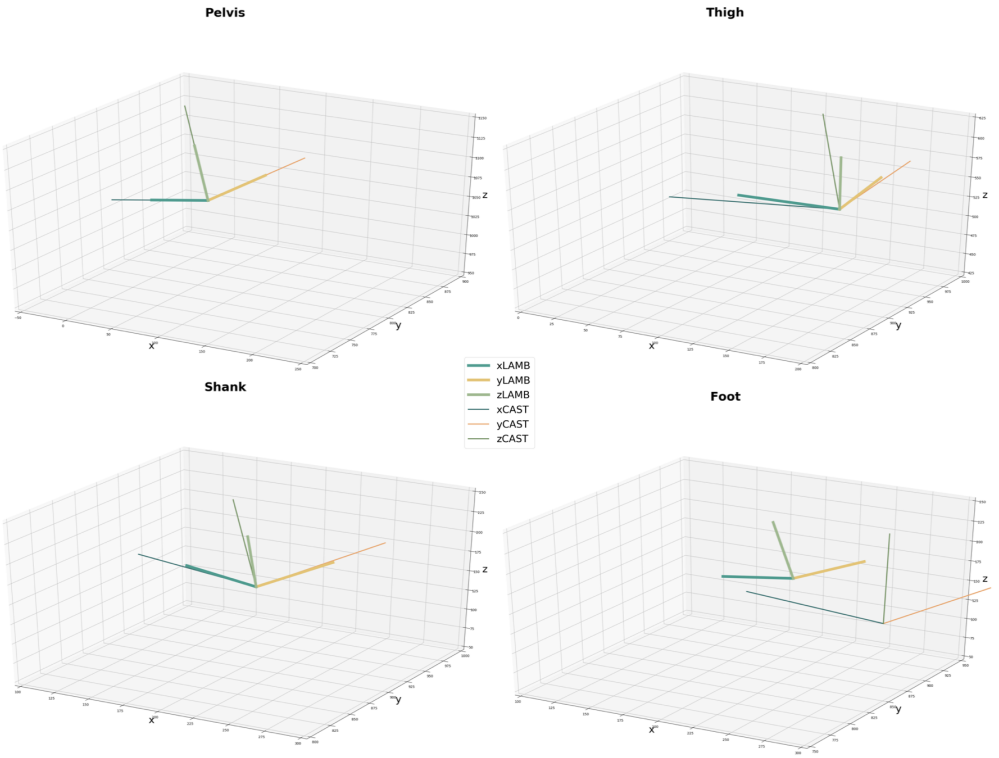

Figure C.7: Anatomical Frames (AFs) for each segment for CAST and LAMB calculated during the calibration trial.

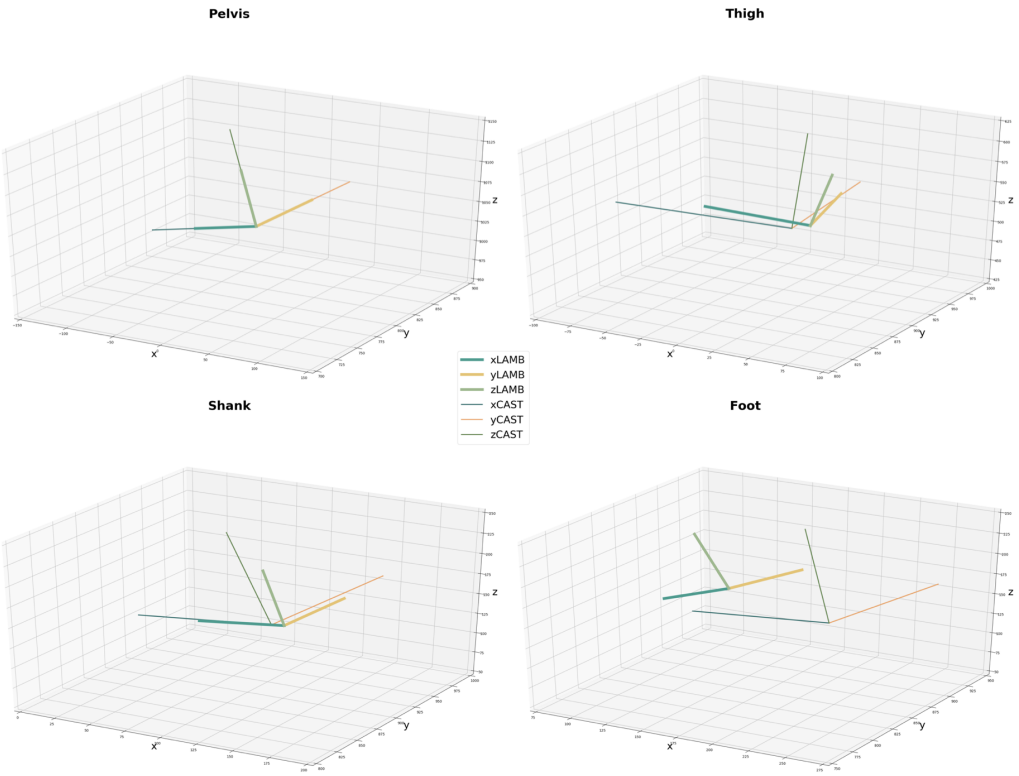

Figure C.8: AFs for each segment for CAST and LAMB calculated during the task trial.

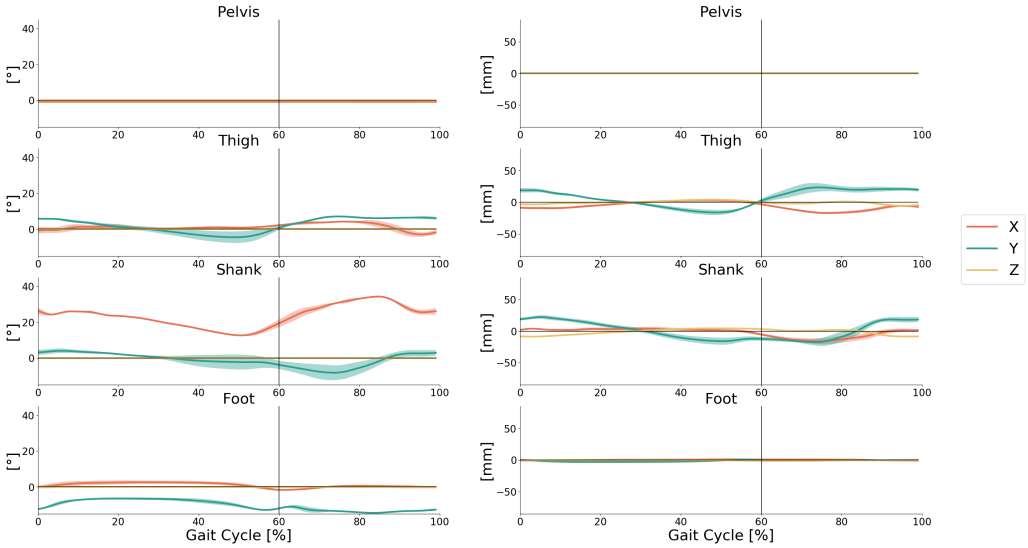

Figure C.9: Rotational and translational offsets between CGM and LAMB AFs for each segment.

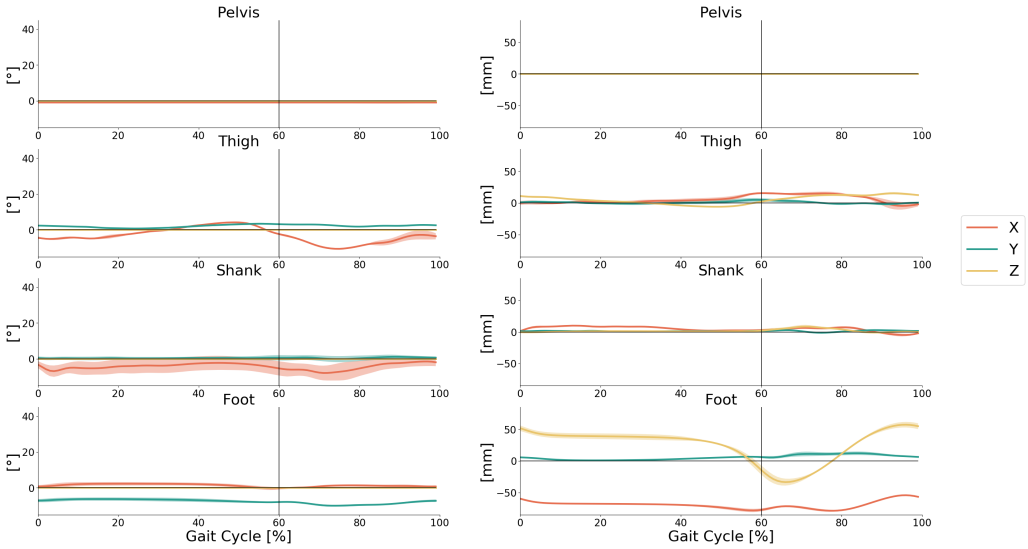

Figure C.10: Rotational and translational offsets between CGM and CAST AFs for each segment.

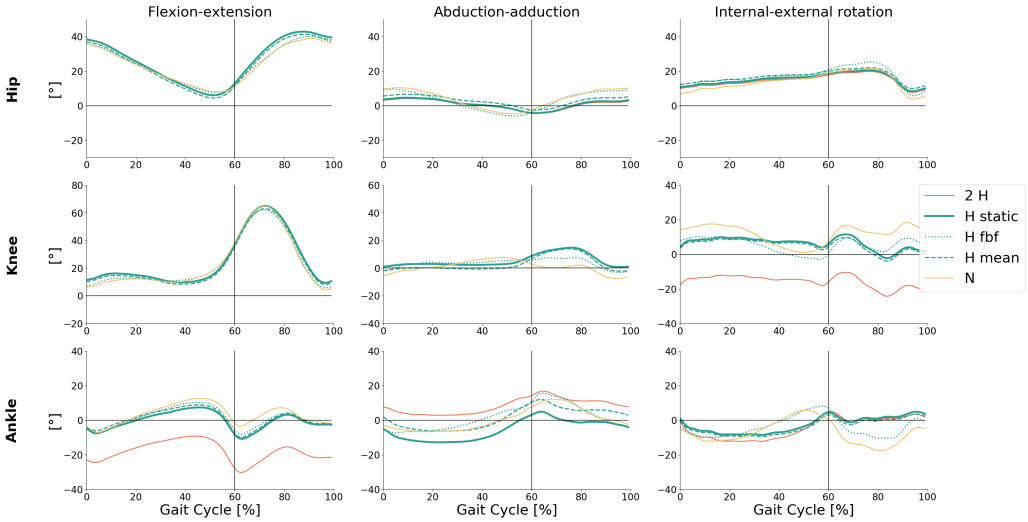

Figure C.11: CT harmonised kinematic curves for the transformation from LAMB to CGM for a typical subject. The red solid line indicates the LAMB native results; the solid yellow line represents the CGM native curves; the blue line are all harmonisations: solid – static uT, dot – frame-by-frame uT and dashed – mean uT.

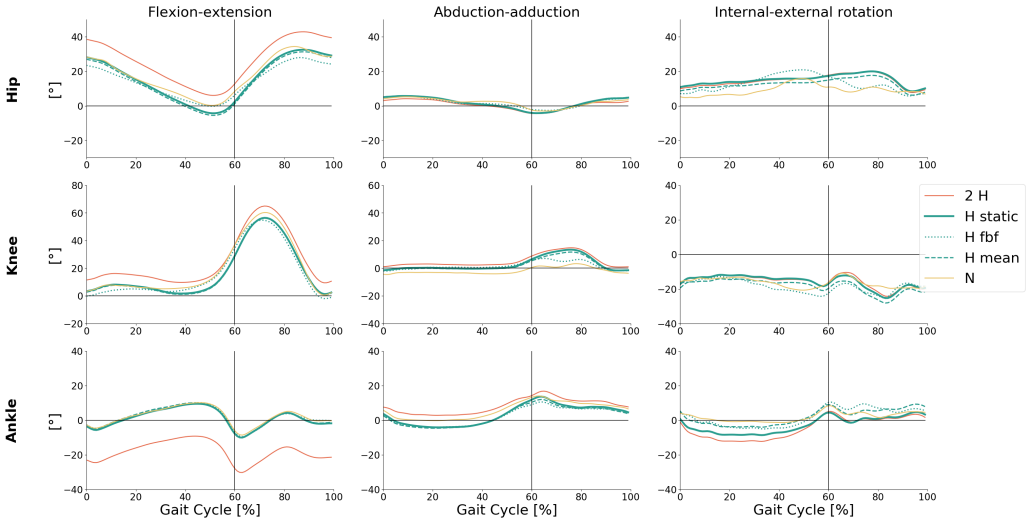

Figure C.12: CT harmonised kinematic curves for the transformation from LAMB to CAST for a typical subject. The red solid line indicates the LAMB native results; the solid yellow line represents the CAST native curves; the blue line are all harmonisations: solid – static uT, dot – frame-by-frame uT and dashed – mean uT.

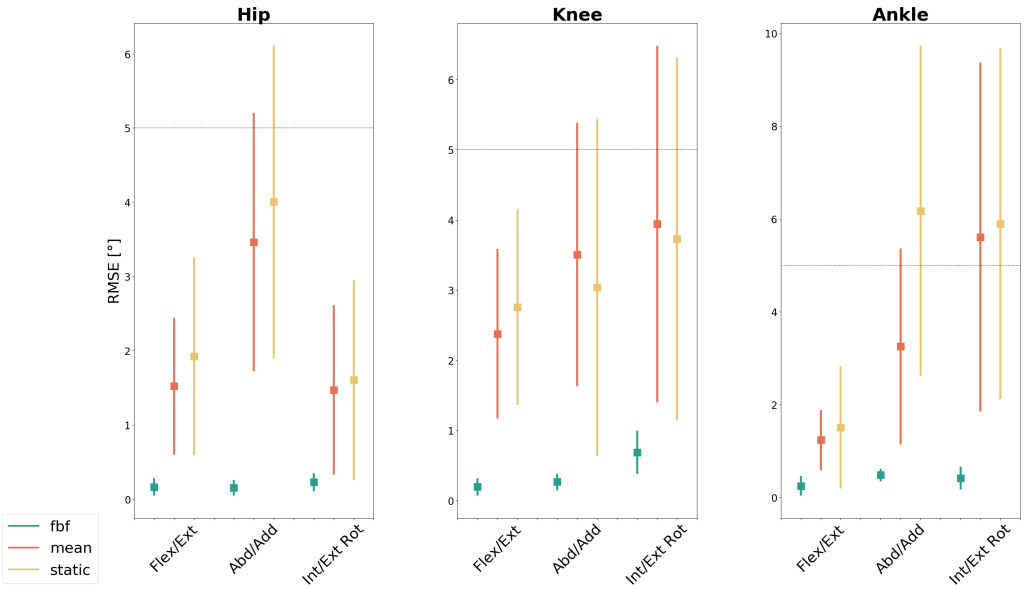

Figure C.13: RMSE between native CGM and CGM harmonised from LAMB.

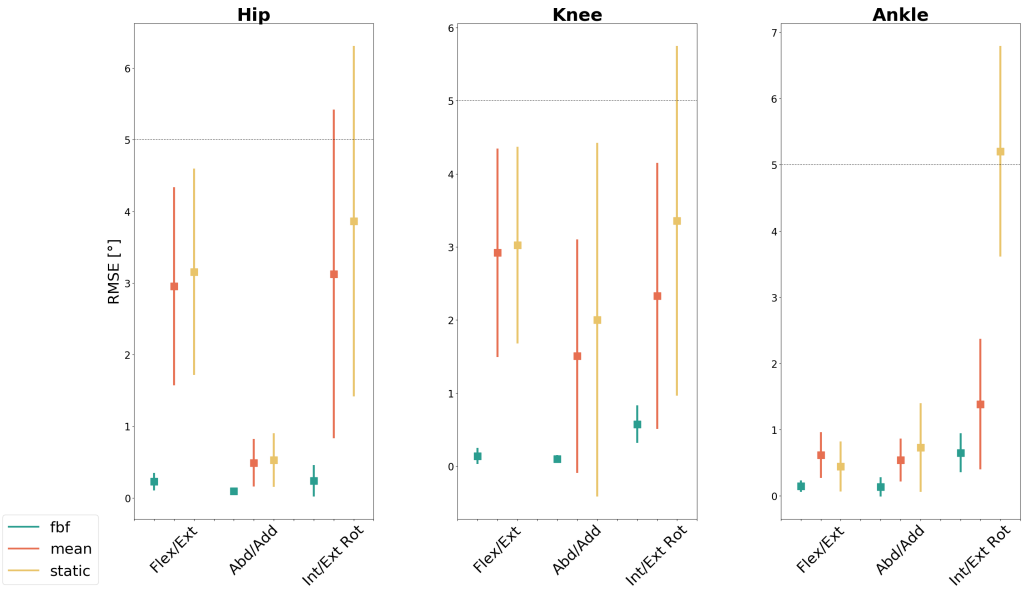

Figure C.14: RMSE between native CAST and CAST harmonised from LAMB.

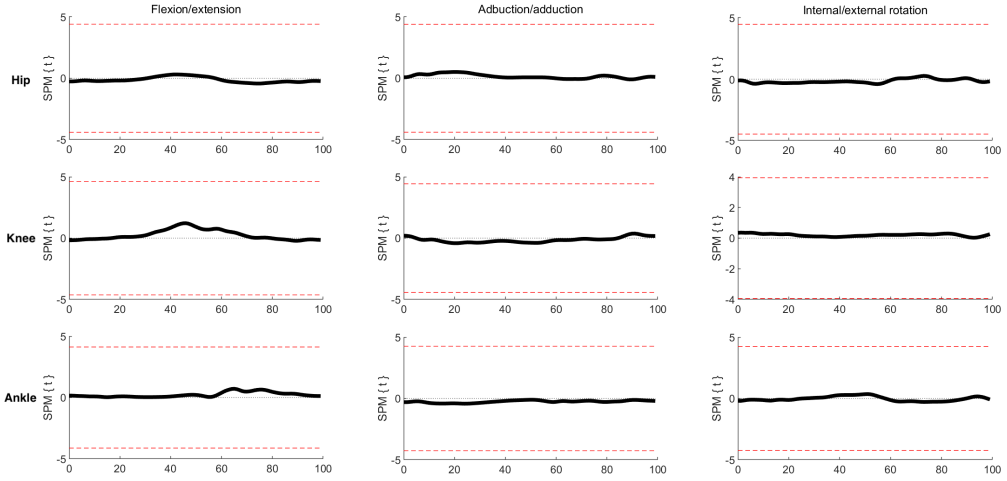

Figure C.15: SPM t-test t-values for CGM harmonised from LAMB with frame-by-frame CT.

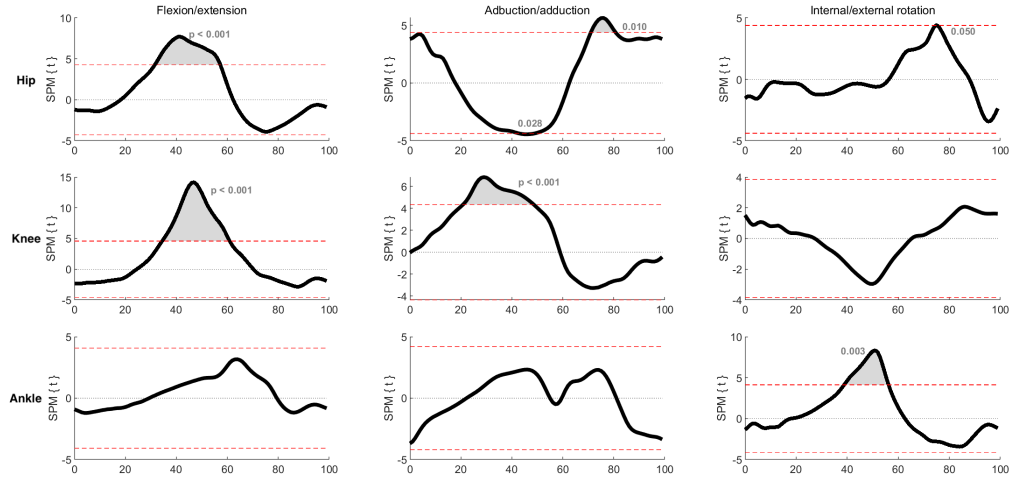

Figure C.16: SPM t-test t-values for CGM harmonised from LAMB with mean CT.

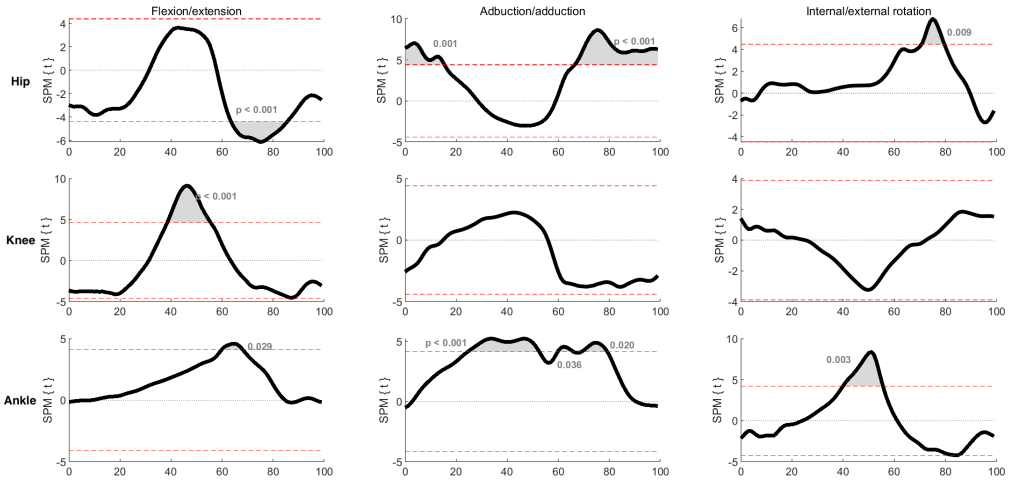

Figure C.17: SPM t-test t-values for CGM harmonised from LAMB with static CT.

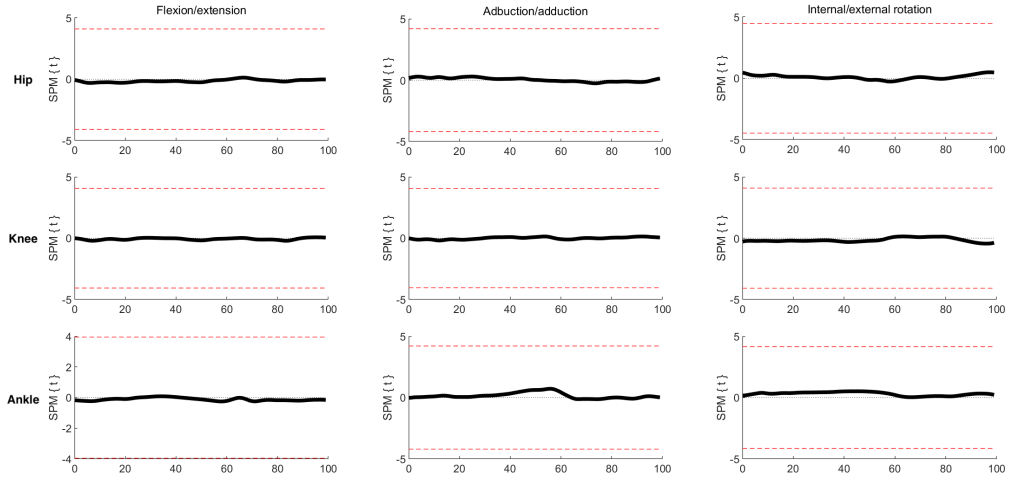

Figure C.18: SPM t-test t-values for CAST harmonised from LAMB with frame-by-frame CT.

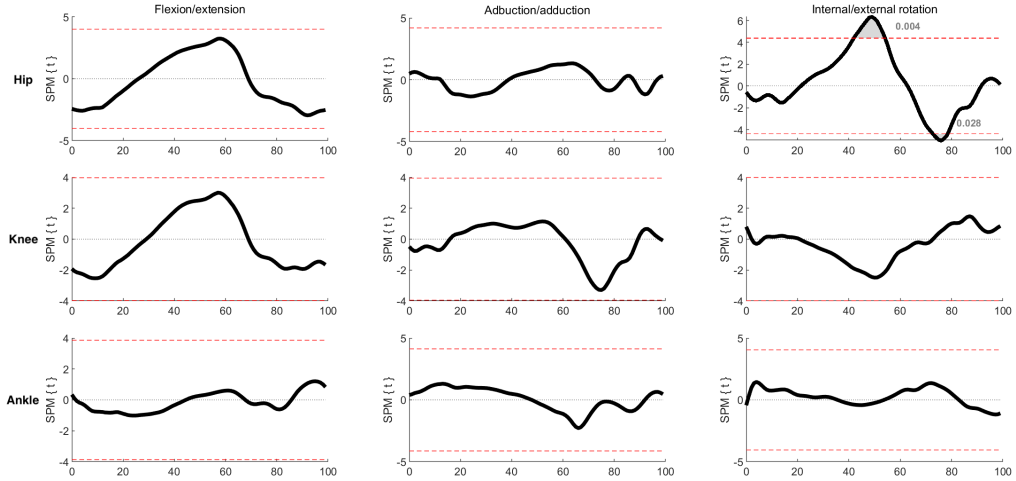

Figure C.19: SPM t-test t-values for CAST harmonised from LAMB with mean CT.

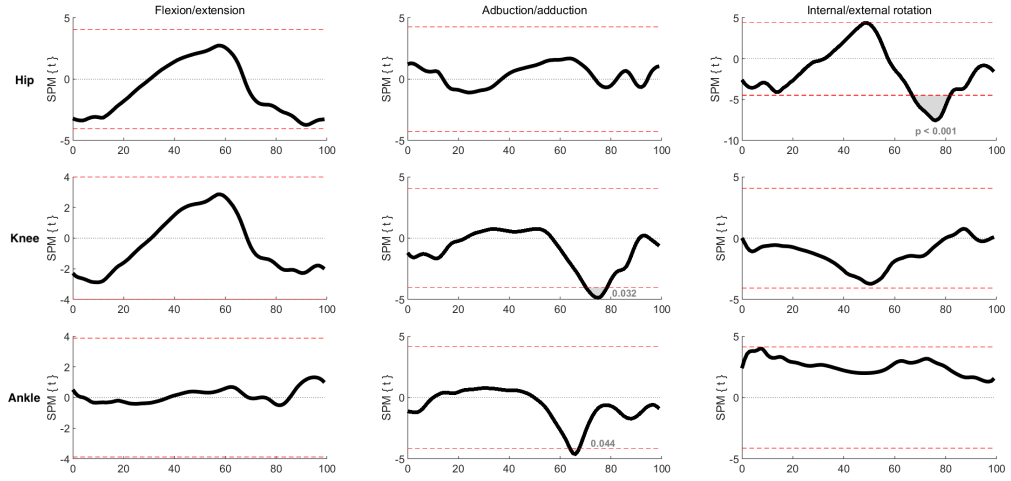

Figure C.20: SPM t-test t-values for CAST harmonised from LAMB with static CT.

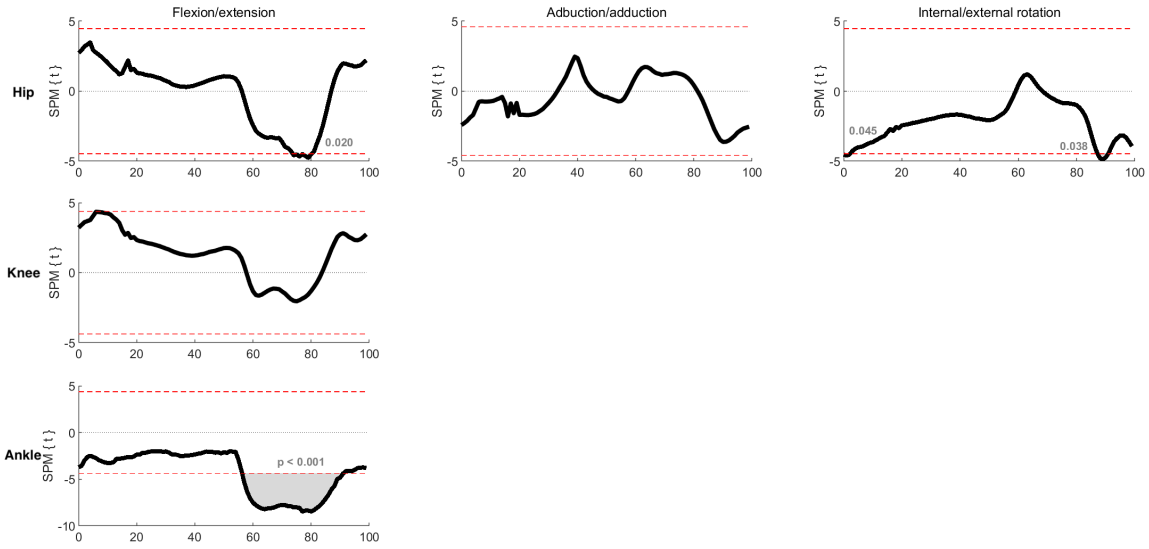

Figure C.21: SPM t-test between IK LAMB and CGM.

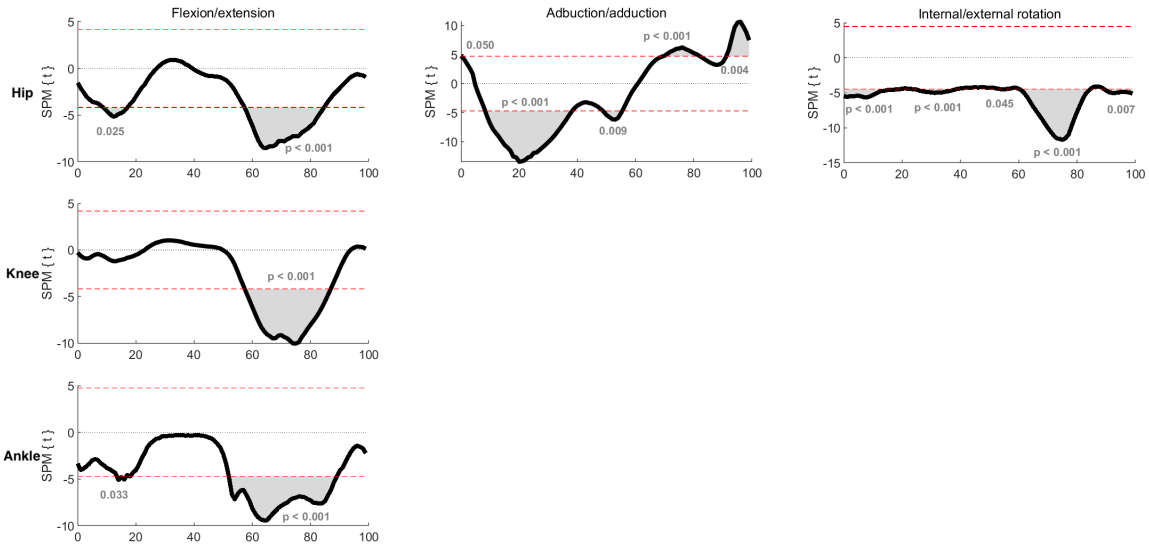

Figure C.22: SPM t-test between IK LAMB and CAST.